Spring 2013

Influence of As(V) on Fe(II)-catalyzed Fe oxide recrystallization

Brittany Huhmann
University of Iowa

INFLUENCE OF AS(V) ON FE(II)-CATALYZED FE OXIDE RECRYSTALLIZATION

by

Brittany Huhmann

A thesis submitted in partial fulfillment
of the requirements for the Master of
Science degree in Civil and Environmental Engineering
in the Graduate College of
The University of Iowa

May 2013

Thesis Supervisor: Professor Michelle M. Scherer

Graduate College
The University of Iowa
Iowa City, Iowa

CERTIFICATE OF APPROVAL

MASTER'S THESIS

This is to certify that the Master's thesis of

Brittany Huhmann

has been approved by the Examining Committee
for the thesis requirement for the Master of Science
degree in Civil and Environmental Engineering at the May 2013 graduation.

Thesis Committee: _____
Michelle M. Scherer, Thesis Supervisor

_____
Gene F. Parkin

_____
David M. Cwiertny

ACKNOWLEDGMENTS

I have learned so much from my advisor, Michelle Scherer, about how to read scientific literature, identify research questions, plan experiments, analyze data, and present the results of my research. She is a highly effective teacher and supervisor, and she has been a role model for me in my own mentoring and leadership activities. I couldn't possibly have hoped for a better and more supportive advisor.

I am also grateful to the other research assistants in Michelle's group for their help with experimental planning, learning laboratory techniques, and troubleshooting problems. Anke Neumann has provided invaluable input, guidance, and encouragement at every step of the research process. Tim Pasakarnis, Dan Allman, Jon Bachman, Jon Sutula, Nick Glynn and many others have also provided assistance at many steps along the way.

I would like to thank Maxim Boyanov, Kenneth Kemner, Bhoopesh Mishra, Drew Latta, and the MRCAT beamline staff at Argonne National Laboratory for assistance with XAS data collection and analysis. I am also grateful to David Peate for his assistance with the ICP-MS.

I am especially thankful for the support of my friends and family. Many thanks to my parents and younger brother for visiting me and making sure I got to explore the area around Iowa City. I am also grateful to my friends at the River City Housing Collective for providing hugs, delicious vegan meals, and much-needed study breaks. The hardest thing about leaving Iowa City will be saying goodbye to all of you! Finally, I am grateful to my partner Matt for his unceasing optimism and encouragement. Thanks for providing feedback on papers, posters, and talks; ideas for negotiating tricky situations; and support when I felt overwhelmed. You have enriched my life in so many ways over the past six years, and I'm fortunate to have you as my best friend.

ABSTRACT

Human exposure to arsenic in groundwater is a global concern, and arsenic mobility in groundwater is often controlled by Fe mineral dissolution and precipitation. Additionally, Fe(II)-catalyzed recrystallization of Fe oxides has been shown to enable trace element release from and incorporation into Fe oxides. However, the effect of As(V) on the Fe(II)-catalyzed recrystallization of Fe oxides such as goethite, magnetite, and ferrihydrite remains unclear. Here, we measured the extent of Fe atom exchange between aqueous Fe(II) and magnetite, goethite, or ferrihydrite in the presence of As(V) by reacting isotopically "normal" Fe oxides with ^{57}Fe-enriched aqueous Fe(II). At lower levels of adsorption (≤ 13.3 μM), As(V) had little influence on the rate or extent of Fe(II)-catalyzed Fe atom exchange in goethite or magnetite. However, Fe atom exchange was increasingly inhibited as As(V) concentration increased above 100 μM. Additionally, adsorbed As(V) may be incorporated into magnetite over time in the presence and absence of added aqueous Fe(II) as indicated by X-ray absorption spectroscopy (XAS) and chemical extraction data, with more rapid incorporation in the absence of added Fe(II). XAS and chemical extraction data are also consistent with the incorporation of As(V) during goethite and magnetite precipitation. Additionally, atom exchange data indicated that low levels of As(V) coprecipitation (As:Fe = 0.0005-0.0155) had little influence on the rate or extent of Fe(II)-catalyzed Fe atom exchange in goethite or magnetite. Atom exchange data indicated that ferrihydrite likely transforms via a dissolution-reprecipitation mechanism both to lepidocrocite at 0.2 mM Fe(II) and to magnetite at 5 mM Fe(II). The presence of 206 μM As(V) slowed the transformation of ferrihydrite to more crystalline iron minerals and slowed the rate of atom exchange between aqueous Fe(II) and ferrihydrite. However, the degree of atom exchange did not directly correlate with the amount of ferrihydrite transformed. In summary, Fe oxide

recrystallization processes may affect As(V) uptake and release in the environment, and As(V) may inhibit Fe(II)-catalyzed Fe oxide recrystallization.

TABLE OF CONTENTS

LIST OF TABLES

LIST OF FIGURES

CHAPTER I. INTRODUCTION

Arsenic in the Environment: A Threat to Human Health

High concentrations of arsenic in groundwater are a global human health threat. The primary route of exposure to inorganic arsenic is through ingestion of contaminated groundwater. Although the toxicity of arsenic is well-known, the mechanism of this toxicity remains poorly understood (*1*). Exposure to arsenic can result in both acute and chronic toxicity, and arsenic poisoning can lead to a wide variety of clinical symptoms. Acute symptoms may include muscular pain, abdominal pain, nausea and vomiting, rashes, intense thirst, confusion, hallucinations, circulatory collapse, and death (*2*). Chronic arsenic poisoning may result in dermatosis, anemia, decreases in white blood cell and platelet count, and increased risk of bladder, lung, and skin cancer (*2*, *3*). Based on these health concerns the World Health Organization has set a guideline value for arsenic of 10 µg/L (0.13 µM) in drinking water, and the United States Environmental Protection Agency has adopted this value as its drinking water standard.

Southeast Asia is the region of the world that has experienced the greatest epidemic of arsenic poisoning; in this region, tens of millions of people are estimated to have been affected (*4*). Arsenic contamination of groundwater is also a cause for concern throughout many other regions of the world, including the United States. In 2000, the United States Geological Survey noted that the new 10 µg/L drinking water standard was exceeded in approximately 10% of the regulated water supplies in the United States (*5*). Arsenic contamination is of particular concern in Iowa, since a 2009 survey of Iowa's well water revealed that 69 public water supplies and 8% of private wells surveyed exceeded the 10 µg/L standard (Figure 1).

Concentrations of arsenic in groundwater vary by more than four orders of magnitude, ranging from less than 0.5 µg/L to more than 5000 µg/L (0.01 – 66.74 µM) (*4*). The source of this arsenic is mainly geogenic, originating from arsenic-containing

minerals in rocks and soils (*4*). Arsenic in the environment may have a range of oxidation states (-3, 0, 3, 5), but arsenic in groundwater is primarily found as arsenite [As(III)] and arsenate [As(V)]. Toxicity studies have demonstrated that arsenite has a greater acute toxicity than arsenate in humans (*6*). Furthermore, arsenite is about an order of magnitude more potent in causing chromosome breakage than arsenate (*6*).

Arsenic speciation and mobility is dependent on groundwater Eh and pH. Arsenic is most commonly present as H_3AsO_3, $H_2AsO_4^-$, and $HAsO_4^{2-}$ at circumneutral pH (Figure 2). Since arsenic is present as an anion, it is more mobile under high-pH conditions when mineral surfaces tend to be more negatively charged. Arsenic is also more mobile under reducing conditions, since arsenite is more soluble and less strongly adsorbed than arsenate (*4*). Arsenic adsorbs more strongly to iron oxides than to most other minerals, and many of the highest arsenic concentrations are found in iron-rich rocks (*4*). The arsenic content of naturally occurring iron oxides ranges widely, from an As:Fe molar ratio of 2.4×10^{-6} to 0.09 (*7*–*9*).

Iron is the element which most strongly correlates with arsenic in sediments, and arsenic mobilization is frequently linked with the desorption/dissolution of arsenic from iron oxides (*4*). Smedley and Kinniburgh (*10*) describe the following five mechanisms by which arsenic may be released into natural waters, all of which frequently involve interactions with iron minerals. (1) Under oxidizing conditions, arsenic is strongly adsorbed to iron oxides at circumneutral pH, but can be rapidly released as the pH increases above 8.5. Such an increase in pH might be caused by the uptake of protons by mineral weathering and ion exchange reactions or by inputs of high-pH geothermal waters. (2) Arsenic mobilization may also be caused by the onset of reducing conditions. For example, the rapid accumulation and burial of sediments can lead to the decomposition of soil organic matter. This can produce reducing conditions under which As(V) is reduced to the more mobile As(III). (3) Arsenic may be mobilized due to a reduction in surface area of oxide minerals. Poorly crystalline, fine-grained iron oxides

with high specific surface areas, such as hydrous ferric oxides (HFOs), are often the first to form during weathering. Over time, HFOs may transform to more crystalline Fe oxides with larger crystallite sizes and lower specific surface areas. This decrease in surface area could, in turn, lead to the desorption of arsenic from iron oxide surfaces. (4) Arsenic release to solution could occur in response to a reduction in binding strength between arsenic and mineral surfaces. For example, under strongly reducing conditions, Fe(III) oxides could be reduced to form mixed-valent oxides such as magnetite and green rust. This would tend to reduce the positive surface charge of the oxide, decreasing its affinity for the negatively charged arsenic ions and resulting in arsenic desorption.

(5) Arsenic may be released by mineral dissolution. For example, dissolution of iron oxides under highly reducing or highly acidic conditions could result in the release of adsorbed or coprecipitated arsenic. The oxidation of arsenic-containing pyrite could also contribute to arsenic mobilization; this process may occur when pyrite is exposed due to a lowering of the water table. In the case of pyrite oxidation, however, if the oxidized iron reprecipitates as iron oxides, these will likely adsorb or incorporate much of the released arsenic, leading to little net release of arsenic to solution.

Iron in the Environment

As the fourth-most abundant element in earth's crust, iron is ubiquitous in natural systems. Iron plays a key role in the chemistry of natural systems, since it may exist in a range of redox states (Fe(0), Fe(II), and Fe(III)) under environmentally relevant conditions. Iron may act as an electron donor (*11*) and electron acceptor in microbial metabolisms (*12*), and iron redox chemistry is linked to the cycling of both nutrients and contaminants (*13*, *14*).

Iron in the environment often exists in the form of iron oxides. Most iron oxides contain iron in the trivalent state, but some iron oxides, such as magnetite, contain Fe(II). In general, iron oxides tend to be colorful, have low solubility, and their structures allow

for the replacement of Fe with other cations (*15*). Due to their high energy of crystallization they tend to form many small crystals, which leads to high specific surface areas, often > 100 m^2/g. This high surface area-to-volume ratio makes them important environmental sorbents for dissolved ions (*15*).

This thesis will focus on the interactions between arsenic and three common iron oxides: goethite, magnetite, and ferrihydrite. Goethite, α-FeOOH, ranges in color from dark brown to ochre. It is one of the most thermodynamically stable iron oxides under environmental conditions, and is often the end member in the transformation of other iron oxides. Magnetite, Fe_3O_4, is a black, ferromagnetic iron oxide containing both Fe(III) and Fe(II). It is most commonly found in anoxic environments and may be an important reductant for environmental contaminants (*16*, *17*). Magnetite can contain varying fractions of Fe(II):

$$x = \frac{\text{Fe(II)}}{\text{Fe(III)}}$$

where x can vary from 0 (completely oxidized) to 0.5 (stoichiometric). Furthermore, the Fe(II) content of magnetite can affect its reactivity (*18*). Ferrihydrite is a reddish-brown iron oxide commonly found in surface environments. It is nanocrystalline and thermodynamically unstable, transforming to more crystalline iron oxides, such as goethite and magnetite, over time (*15*). The rate and end products of ferrihydrite transformation are affected by temperature, pH, aqueous Fe(II) concentration, and concentrations of other ions (*19*, *20*).

Fe(II)-Catalyzed Recrystallization of Fe Oxides

Iron redox chemistry plays a key role in the environmental cycling of many elements, including arsenic. An important aspect of this redox chemistry is the Fe(II)-catalyzed recrystallization of Fe oxides. Fe(II)-catalyzed recrystallization is commonly observed for unstable Fe oxides such as lepidocrocite and ferrihydrite, which transform to

more stable Fe oxides such as goethite and magnetite (*19*, *21*). In contrast, aqueous Fe(II) was historically believed to interact with more stable iron oxides only by adsorption and desorption from the surface. However, it has recently been demonstrated that adsorbed Fe(II) can transfer an electron into Fe(III) or mixed-valent Fe oxides (*22*). This process of electron transfer has been observed to occur between aqueous Fe(II) and goethite (*22*), hematite (*22*), and magnetite (*23*). Electron transfer has also been observed between Fe(II) and the unstable Fe oxide ferrihydrite (*22*).

Recent research has demonstrated that this process of electron transfer is accompanied by atom exchange between the Fe(II) in the aqueous phase and the Fe in the mineral. Under some conditions complete mixing between the two pools of iron has been observed, indicating a complete recrystallization of the Fe oxide (*24*). This process of atom exchange has been observed between aqueous Fe(II) and goethite (*24*) and magnetite (*25*). Atom exchange has also been observed between aqueous Fe(II) and the unstable Fe oxides ferrihydrite (*26*, *27*) and lepidocrocite (*27*) during the Fe(II)-catalyzed transformation of these minerals. In contrast, atom exchange was not observed between aqueous Fe(II) and hematite (*28*), even though electron transfer between aqueous Fe(II) and hematite has been observed (*22*).

Three different mechanisms have been proposed to explain the observed atom exchange between aqueous Fe(II) and stable Fe oxides (*24*). Solid state diffusion of Fe within the crystal lattice is one potential mechanism. In the case of goethite, this mechanism can be ruled out, since diffusion rates are much too slow to account for the observed rate of exchange. Nearly complete atom exchange between aqueous Fe(II) and goethite was observed over 10 days, whereas achieving complete exchange via solid-state diffusion would require time scales on the order of millions of years (*24*, *28*). In contrast, solid state diffusion could account for the observed rates of atom exchange in magnetite. Diffusion rates for magnetite are thought to be much faster than those for goethite (*29*–*33*). Reported diffusion coefficients for magnetite vary widely, but even the more

conservative rates reported could account for the observed rate of atom exchange (55-63% in 30 days) (*34*).

Diffusion through micropores is another potential mechanism for the atom exchange observed between stable Fe oxides and aqueous Fe(II), since the rate of diffusion through micropores could be much more rapid than solid-state diffusion. However, the fact that aqueous Fe(II) concentrations remain constant after initial Fe(II) sorption to the goethite or magnetite suggests that pore diffusion is an unlikely explanation (*24*, *34*).

A final proposed mechanism is the "redox-driven conveyor belt" model of atom exchange (Figure 3). It has been observed that a potential gradient between two different crystal faces of hematite can result in bulk conduction through the hematite, leading to dissolution on one face coupled with oxide growth on the other (*35*). A similar mechanism may be responsible for the atom exchange observed between magnetite or goethite and aqueous Fe(II). In this mechanism, an aqueous Fe(II) atom is adsorbed to the surface of an iron mineral and an electron is transferred into the bulk mineral, resulting in growth of the iron oxide at the site of electron transfer. The electron is then conducted through the bulk mineral until it reaches a different site on the mineral surface, where it reduces a surface Fe(III) to Fe(II), and the reduced atom is released to the solution (*24*). As this process continues over time, most or all of the Fe atoms could eventually be exposed to the aqueous phase and exchanged.

Contaminant Uptake and Release during Fe(II)-Catalyzed Fe Oxide Recrystallization

As a result of Fe(II)-catalyzed Fe oxide recrystallization, Fe oxides are capable of structurally incorporating and releasing trace elements. Incorporation of As(V) during the Fe(II)-catalyzed recrystallization of ferrihydrite and lepidocrocite to more stable Fe oxides has been hypothesized based on chemical extraction data (*27*). Furthermore,

incorporation of As(V) into magnetite during the transformation of lepidocrocite and ferrihydrite to magnetite has been hypothesized based on X-ray absorption spectroscopy (XAS) on the As(V) coordination (*36*, *37*) and X-ray magnetic circular dichroism (XMCD) evidence of distortion of the magnetite structure due to As(V) incorporation (*37*). Additionally, incorporation of U during Fe(II)-catalyzed recrystallization of ferrihydrite has been hypothesized based on XAS (*38*, *39*).

Incorporation and release of trace elements from stable iron oxides in the presence of Fe(II) has also been observed. For example, incorporation of Ni into hematite (*40*) and Tc(IV) into goethite (*41*) in the presence of Fe(II) has been hypothesized based on XAS. Additionally, release of Ni and Zn from Ni- and Zn-substituted goethite and hematite (*40*, *42*), release of Mn from Mn-substituted goethite (*43*), and release of Co from Co-ferrite (a mineral isomorphic with magnetite, where Fe(II) is replaced by Co^{2+}) (*25*) in the presence of Fe(II) has also been observed. In contrast, XAS data suggest that As(V) remained adsorbed or precipitated as ferrous arsenate rather than being incorporated into goethite or hematite in the presence of Fe(II) (*44*).

Objectives and Hypotheses

The two objectives of this study were as follows: 1) Investigate the influence of As(V) on the rate and extent of the Fe(II)-catalyzed recrystallization of stable and unstable Fe oxides, and 2) Investigate whether As(V) is incorporated or released during Fe(II)-catalyzed Fe oxide recrystallization. According to these objectives, the following hypotheses were developed:

1. The presence of adsorbed As(V) will decrease the rate and extent of Fe atom exchange between aqueous Fe(II) and the Fe oxides goethite, magnetite, and ferrihydrite.
2. Adsorbed As(V) will be incorporated into the mineral structure during the Fe(II)-catalyzed recrystallization of goethite and magnetite.

3. As(V) will be structurally incorporated when goethite and magnetite are precipitated in the presence of As(V).
4. As(V) will be redistributed to the mineral surface during the Fe(II)-catalyzed recrystallization of goethite and magnetite with pre-incorporated As(V).

Thesis Overview

Chapter II addresses the above hypotheses. Chapter III summarizes the engineering and scientific significance of the work performed in Chapter II.

Chapter II examines the effect of As(V) on the Fe(II)-catalyzed recrystallization of Fe oxides such as goethite, magnetite, and ferrihydrite, as well as the fate of As(V) during this recrystallization. As(V) was selected, as it generally is not abiotically reduced by Fe(II) (*45*); in contrast, As(III) can be oxidized in such systems (*46*). We measured the extent of Fe atom exchange between aqueous Fe(II) and magnetite, goethite, or ferrihydrite in the presence of As(V) by reacting isotopically "normal" Fe oxides with ^{57}Fe-enriched aqueous Fe(II). At low concentrations ($\leq$ 13.3 μM), adsorbed As(V) had little influence on the rate or extent of Fe(II)-catalyzed Fe atom exchange in goethite or magnetite; however, Fe atom exchange between aqueous Fe(II) and goethite and magnetite was increasingly inhibited as As(V) concentration increased above 100 μM. Coprecipitation of As(V) with goethite and magnetite was not observed to inhibit Fe atom exchange.

Chemical extractions of the As(V) provide little evidence for As(V) incorporation or redistribution during Fe(II)-catalyzed recrystallization of goethite or magnetite on timescales of a few days. However, our data indicate that As(V) incorporation during Fe(II)-catalyzed recrystallization of magnetite may occur over significantly longer timescales than atom exchange. Additionally, XAS data indicate that As(V) may be progressively incorporated into magnetite at long adsorption times in the absence of

aqueous Fe(II), which may be due to the dissolution of small amounts of Fe(II) from magnetite followed by Fe(II)-catalyzed magnetite recrystallization. In contrast, XAS data indicate that arsenic remains adsorbed on the goethite surface even at long adsorption times.

Atom exchange data indicate that ferrihydrite transforms via a dissolution-reprecipitation mechanism both to lepidocrocite at 0.2 mM Fe(II) and to magnetite at 5 mM Fe(II). The presence of 206 μM As(V) slowed both the transformation of ferrihydrite to more crystalline iron minerals and the rate of atom exchange between aqueous Fe(II) and ferrihydrite. However, the degree of isotope exchange did not directly correlate with the amount of ferrihydrite transformed. This work shows that As(V) may inhibit Fe(II)-catalyzed Fe oxide recrystallization and suggests that these recrystallization processes may affect As(V) uptake and release in the environment.

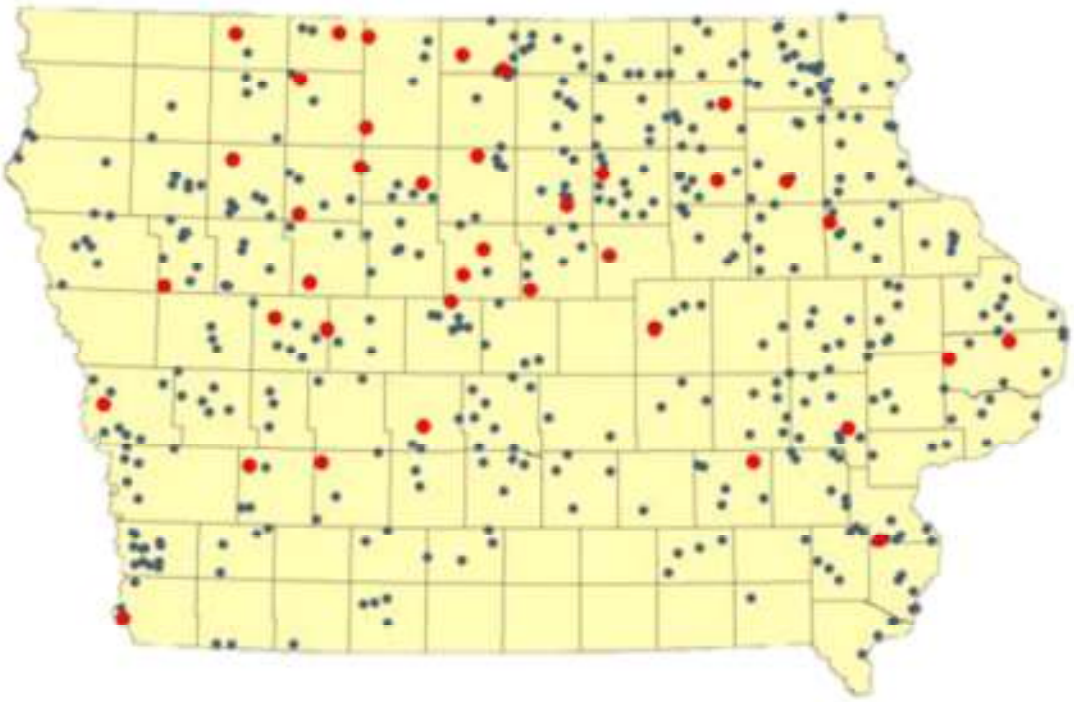

Figure 1 Arsenic in Iowa private wells. Wells in red contain arsenic concentrations above the EPA limit of 10 µg/L (*47*).

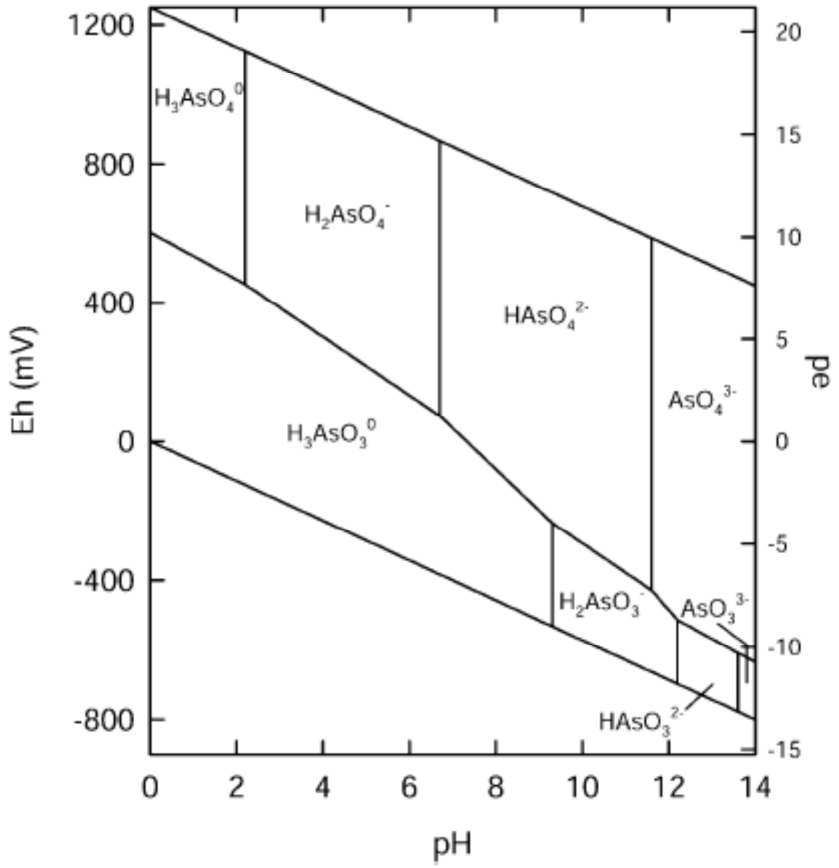

Figure 2 Eh-pH diagram for aqueous arsenic in the system As-O_2-H_2O at 25°C and 1 bar total pressure (*4*).

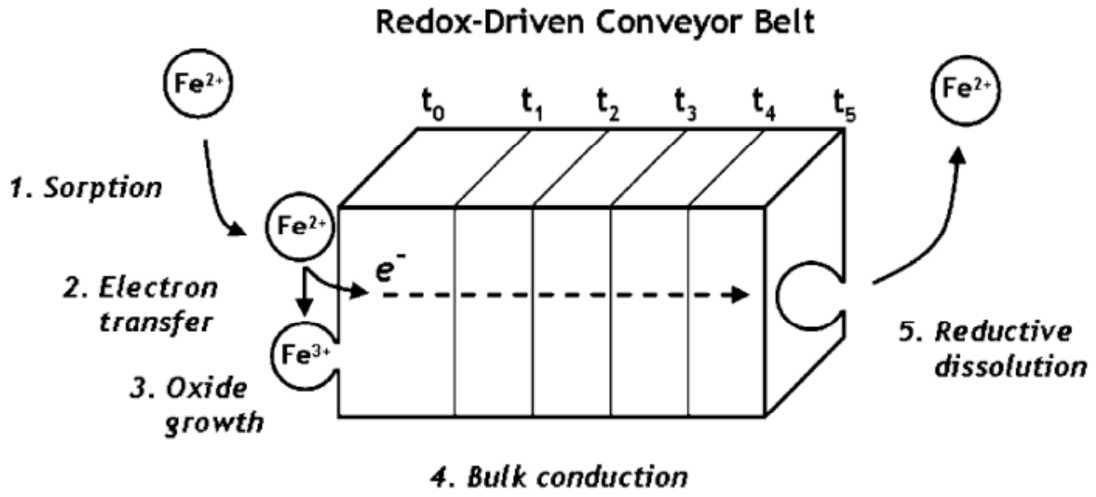

Figure 3 The redox-driven conveyor belt conceptual model for electron transfer and atom exchange (*24*).

CHAPTER II: INFLUENCE OF AS(V) ON FE(II)-CATALYZED FE OXIDE TRANSFORMATIONS

Abstract

Human exposure to arsenic in groundwater is a global concern, and arsenic mobility in groundwater is often controlled by Fe mineral dissolution and precipitation. Additionally, Fe(II)-catalyzed recrystallization of Fe oxides has been shown to enable trace element release from and incorporation into Fe oxides. However, the effect of As(V) on the Fe(II)-catalyzed recrystallization of Fe oxides such as goethite, magnetite, and ferrihydrite remains unclear. Here, we measured the extent of Fe atom exchange between aqueous Fe(II) and magnetite, goethite, or ferrihydrite in the presence of As(V) by reacting isotopically "normal" Fe oxides with ^{57}Fe-enriched aqueous Fe(II). At lower levels of adsorption (≤ 13.3 μM), As(V) had little influence on the rate or extent of Fe(II)-catalyzed Fe atom exchange in goethite or magnetite. However, Fe atom exchange was increasingly inhibited as As(V) concentration increased above 100 μM. Additionally, adsorbed As(V) may be incorporated into magnetite over time in the presence and absence of added aqueous Fe(II) as indicated by X-ray absorption spectroscopy (XAS) and chemical extraction data, with more rapid incorporation in the absence of added Fe(II). XAS and chemical extraction data are also consistent with the incorporation of As(V) during goethite and magnetite precipitation. Additionally, atom exchange data indicated that low levels of As(V) coprecipitation (As:Fe = 0.0005-0.0155) had little influence on the rate or extent of Fe(II)-catalyzed Fe atom exchange in goethite or magnetite. Atom exchange data indicated that ferrihydrite likely transforms via a dissolution-reprecipitation mechanism both to lepidocrocite at 0.2 mM Fe(II) and to magnetite at 5 mM Fe(II). The presence of 206 μM As(V) slowed the transformation of ferrihydrite to more crystalline iron minerals and slowed the rate of atom exchange between aqueous Fe(II) and ferrihydrite. However, the degree of atom exchange did not directly correlate with the amount of ferrihydrite transformed. In summary, Fe oxide

recrystallization processes may affect As(V) uptake and release in the environment, and As(V) may inhibit Fe(II)-catalyzed Fe oxide recrystallization.

Experimental Methods

All experiments were conducted in a 93:7 N_2:H_2 anaerobic glovebox (O_2 < 1 ppm) unless otherwise noted. All solutions were purged with N_2 for at least one hour prior to introduction into the glovebox, where they were allowed to equilibrate with the glovebox atmosphere overnight prior to use. All reactors were covered in aluminum foil to avoid photochemical reactions.

Mineral Synthesis and Characterization

The nanometer-sized goethite (nanogoethite) used in the atom exchange experiments in the presence of adsorbed As(V) was synthesized according to methods described previously, and is a modification of procedures described by Burleson and Penn (*48*, *49*). After synthesis, the nanogoethite was ground and sieved through a 45 micron sieve. The micrometer-sized goethite (microgoethite) used in the atom exchange experiment analogous to the conditions of Catalano *et al.* (*50*) was synthesized according to Schwertmann and Cornell's method for the preparation of goethite from Fe(III) systems (*51*). After synthesis, the microgoethite was ground and sieved through a 150 micron sieve. Poorly crystalline As-free and As-coprecipitated goethite used in the atom exchange experiments was prepared from Fe(II) according to the method described in Pedersen *et al.* (*52*) which is adapted from Schwertmann and Cornell (*51*). For the As-coprecipitated goethite, As:Fe mole ratios measured by dissolution were 0.0008, 0.0015, and 0.0155. For all synthesis methods, goethite was the only phase detected using powder X-ray diffraction (pXRD) (Figure 4). XRD measurements of all minerals were made with a Rigaku MiniFlex II diffractometer using Co-Kα radiation.

Magnetite batches were synthesized in an anaerobic chamber as previously described (*53*). Briefly, isotopically-normal Fe(II) and Fe(III) were combined at a 1:2

ratio in deionized water (added as $FeCl_2$ and $FeCl_3 \cdot 6H_2O$, respectively) before raising the solution pH to 10-11 with NaOH. Magnetite precipitates were aged in anoxic suspension for 24 hr. Previous work with this magnetite synthesis method has reliably produced magnetite batches of relatively uniform particle morphology (*18*, *54*). For As-coprecipitated magnetite, As(V) was added before the pH was raised to begin magnetite precipitation, similar to the method described in Wang *et al.* (*55*). As:Fe mole ratios measured by dissolution were 0.0005, 0.0010, and 0.0099. After synthesis, the magnetite was ground and sieved through a 150 micron sieve. XRD samples were prepared by mixing magnetite solids with a small amount of glycerol to prevent oxidation during the measurement, and for all synthesis methods, magnetite was the only phase detected using pXRD (Figure 5). The stoichiometry of each batch was determined by dissolving pre-weighed samples in 5 M HCl in an anaerobic glovebox (*54*). Fe(II) and total Fe were measured colorimetrically using the phenanthroline method, as previously described (*18*, *54*).

Ferrihydrite was synthesized according to Wilkie and Hering (*56*). Synthesis parameters and characterization for all minerals can be found in Table 1.

Isotope Exchange Experiments

Isotope exchange experiments were conducted using aqueous $^{57}Fe(II)$ and goethite, magnetite, or ferrihydrite with a natural isotope composition. For the nanogoethite experiments, an aliquot of the $^{57}FeCl_2$ solution was added to give an approximate concentration of 1 mM Fe(II) in 15 mL of 25 mM HEPES buffer containing 25 mM KBr as a supporting electrolyte, and the pH was adjusted back to a value of 7.5 with a small volume of NaOH. Then, 30 mg (±0.1 mg) of goethite was added to initiate the reaction (giving a solids concentration of 2 g/L). Triplicate 30 mL Oak Ridge style centrifuge tube reactors were allowed to react for 10 min to 7 days on a rotator in the anoxic chamber. After the reaction, the solution pH was measured, and the centrifuge

tubes were sealed with an O-ring and Teflon tape. The reactors were centrifuged outside the glovebox at 13,000 × g for 15 min and immediately returned to the glovebox. The supernatant was decanted off the pelleted goethite, filtered past a 0.22 μm filter, and acidified with 50 μL of concentrated HCl. The pellet was dissolved in 5 mL of concentrated HCl.

The experiments on poorly crystalline goethite with and without pre-incorporated As(V) were conducted similarly; however, due to higher Fe(II) adsorption to this goethite, the experiment was conducted with a 25 mM PIPES buffer at pH 6.5. Additionally, for the experiment under the conditions of Catalano et al. (*50*), microgoethite was used, and the experiment was conducted in a pH 6.0 solution of 1 mM MES with a solids concentration 4 g/L.

For the atom exchange experiments on magnetite with and without pre-incorporated As(V), the solution was buffered at pH 7.2 with 50 mM MOPS, and a solids loading of 1 g/L magnetite was used. Additionally, the magnetite solids were dissolved in 5 mL of 5 M HCl. For the atom exchange experiments with adsorbed As(V) on goethite or magnetite, the Fe oxide was first allowed to equilibrate with the buffered solution overnight. An aliquot of As(V) stock solution was then added to give the desired As(V) concentration, and the As(V) was allowed to adsorb to the mineral for at least 5 hours before the ^{57}Fe(II) was added to start the experiment.

Finally, for the atom exchange experiments on ferrihydrite, the solution was buffered at pH 7.2 with 50 mM MOPS, although a pH decline of up to 0.65 units was observed due to proton release during mineral transformation under some reaction conditions. A solids loading of 0.5 g/L was used, and an aliquot of $^{57}Fe(II)Cl_2$ solution was added to give an approximate concentration of 0.2 mM Fe(II) or 5.0 mM Fe(II). At the end of the experiment the solids were dissolved in 5 mL of concentrated HCl. For the atom exchange experiments in the presence of adsorbed As(V), the ferrihydrite was added directly to a solution containing Fe(II) and As(V) to start the experiment. A

duplicate set of experiments with Fe(II) of natural isotope composition was conducted under all conditions so that the transformation products could be measured by pXRD.

After each experiment was completed, Fe(II) was measured using 1,10-phenanthroline with masking of Fe(III) by fluoride (*57*). Total Fe was measured by reduction of Fe(III) by hydroxylamine hydrochloride to Fe(II). Isotope analysis was performed with a Thermo Fisher Scientific X Series 2 Quadrupole Inductively Coupled Plasma-Mass Spectrometer (ICP-MS) operating in collision cell mode with a glass concentric nebulizer and a HEPA filtered autosampler. Collision cell gas was 7% H_2, 93% He (>99.996% pure) with a flow rate of about 4 mL min^{-1} to remove the isobaric interference of $^{16}O^{40}Ar$ with ^{56}Fe. Aqueous and solid phase Fe isotope measurements were done by diluting to a total Fe concentration of 0.448-0.627 μM in 0.45 M HNO_3. Dilution kept the signal on all Fe isotopes in the pulse-counting mode on the mass detector and avoided linearity issues in converting the signal response between pulse-counting and analog voltage detection modes. Changes in instrumental detection efficiency were monitored using an internal spike of 30 ppb ^{59}Co. ^{59}Co counts varied by 20-25% over the course of a run. However, since the purpose of the ICP-MS measurements was to determine relative iron isotope abundance within each sample, between-sample variability in detection efficiency should have no impact on our Fe atom exchange calculations. Fe isotope fractions were calculated by dividing the counts in each isotope channel by the sum of the total counts over all four channels (masses of 54, 56, 57, and 58). The fractional isotopic composition for isotope *i* is given by:

$$f^{i}\mathrm{Fe} = \frac{^{i}\mathrm{counts}}{^{54}\mathrm{counts} + ^{56}\mathrm{counts} + ^{57}\mathrm{counts} + ^{58}\mathrm{counts}}.$$

As(V) Extraction Experiments

As(V) extraction experiments were conducted to differentiate between surface-bound and occluded/incorporated As(V) following precipitation or Fe(II)-catalyzed

recrystallization of magnetite or goethite. To extract the adsorbed As(V), 1 g/L magnetite or 2 g/L goethite was added to 1 M NaOH in triplicate Oak Ridge style centrifuge tube reactors and allowed to react for 4 hours on a rotator in the anaerobic chamber. The reactors were then centrifuged and the aqueous phase decanted as previously described for the atom exchange experiments. This was followed by a second, 20-hour extraction with 1 M NaOH, and the solution was again centrifuged and the aqueous phase decanted. The remaining solids were dissolved in 5 mL of 5 M HCl (magnetite) or concentrated HCl (goethite).

Fe concentrations were measured by the phenanthroline method (*57*) and showed that less than 1% of the Fe was extracted by the NaOH (data not shown). As(V) concentrations were measured in collision-cell mode on the ICP-MS, to remove the isobaric interference of $^{40}Ar^{35}Cl$ with ^{75}As. Samples were diluted such that arsenic concentrations were measured in the range of 0 – 5 μM. Formation of $^{40}Ar^{37}Cl$ (^{77}Se) was monitored to account for the potential interference of $^{40}Ar^{35}Cl$ with ^{75}As. The formation of $^{40}Ar^{37}Cl$ was generally low, indicating little interference for most samples. The following correction factor was applied to account for the $^{40}Ar^{35}Cl$ interference (*58*, *59*):

$$As_{calculated} = As_{measured} - 3.13 \times {}^{77}Se$$

Changes in instrumental detection efficiency were monitored using an internal spike of 30 ppb of ^{59}Co and 10 ppb of ^{89}Y. Since instrumental detection efficiency varied over the course of a run, arsenic counts were adjusted according to the following equation:

$$As_{calculated} = As_{measured} \times \frac{Y_{average}}{Y_{measured}}.$$

X-ray Absorption Spectroscopy

Samples of As(V) adsorbed on goethite and magnetite in the absence of Fe(II), adsorbed on magnetite in the presence of Fe(II), and coprecipitated with goethite and

magnetite were measured by X-ray absorption spectroscopy (XAS). The XAS measurements were made at the Materials Research Collaborative Access Team (MRCAT) beamline at the Advanced Photon Source at Argonne National Laboratory.

Results and Discussion

Effect of As(V) on Fe(II)-catalyzed recrystallization of magnetite

To determine whether arsenate influences Fe(II)-catalyzed recrystallization of magnetite, we measured the extent of Fe atom exchange when arsenate was both adsorbed to magnetite and coprecipitated with magnetite. Previous work has shown that the presence of increasing concentrations of adsorbed As(V) decreases the rate and extent of Fe(II)-catalyzed transformation of ferrihydrite (*60*). Since adsorbed As(V) is observed to inhibit the recrystallization of this unstable Fe oxide, we hypothesized that adsorbed As(V) would also inhibit Fe(II)-catalyzed recrystallization of stable Fe oxides such as magnetite. We therefore hypothesized that the presence of adsorbed As(V) on magnetite would inhibit atom exchange between Fe(II) and magnetite.

We measured Fe atom exchange using an enriched Fe isotope tracer approach similar to our previous work (*24*, *34*). We reacted an aqueous solution enriched with ^{57}Fe(II) with a suspension of magnetite having a natural isotope composition and tracked the change in the isotope composition of the aqueous and solid phases with time. Consistent with our previous work (*34*), the fraction of ^{57}Fe ($f^{57}\text{Fe} = {}^{57}\text{Fe}/\Sigma\text{Fe}$) in the aqueous phase decreases substantially over time while the fraction in the solid phase (solids + Fe(II) taken up by the solids) increases, indicating that magnetite in the absence of As(V) undergoes significant Fe atom exchange (Figure 6 and Table 2).

Magnetite was then reacted with Fe(II) in the presence of pre-adsorbed 13.3 μM As(V) for 7 days to investigate the influence of adsorbed As(V). This arsenic concentration is 100-fold greater than the EPA's drinking water standard of 0.133 μM. It

is within the range of arsenic concentrations observed in natural waters (<0.01 μM to >66.74 μM) but is a higher concentration than is typical for most natural waters (*4*). Similar studies of the effect of As(V) on Fe oxide recrystallization have used As concentrations in the range of 50 – 1100 μM (*50*, *60*). At our 13.3 μM arsenic loading and pH of 7.2, near-complete adsorption of the As(V) was observed, which is consistent with previous observations of significant As(V) adsorption on magnetite at circumneutral pH (*61*). Under these conditions, the magnetite is far from surface saturation, which we observed only after As(V) at an initial concentration of 300 μM was added to the system (Figure 7). The presence of adsorbed As(V) at this concentration showed little effect on the change in ^{57}Fe enrichment in the aqueous and solid phases over time, indicating negligible influence on the extent of Fe atom exchange (Figure 6).

To quantify the extent of Fe atom exchange between the aqueous Fe(II) and magnetite solids, we used:

$$\text{Percent exchange} = \frac{f_t - f_i}{f_e - f_i} \times 100, \text{ where } f = {}^{57}\text{Fe}/\Sigma\text{Fe}.$$

Here, f_t is the isotopic composition (as measured by f^{57}Fe = ^{57}Fe/ΣFe) at time t, f_i is the initial isotopic composition, and f_e is the equilibrium isotopic composition of the phase of interest (*62*). As we noted previously, sorption of ^{57}Fe(II) onto magnetite biases the solid phase toward a heavier composition (*25*). Because of the bias in the solid-phase f^{57}Fe, we use the aqueous phase f^{57}Fe to calculate atom exchange at the end of 7 days, which indicates 58.5 ± 6.7 percent exchange in the absence of As(V) and 61.2 ± 2.3 percent exchange after reaction with 13.3 μM As(V). These results are consistent with previous observations of atom exchange between aqueous Fe(II) and magnetite, where 52.5 percent exchanged after 6 days and 55.3 percent exchanged after 30 days under similar conditions to our As-free experiment (*34*). As we have in previous work (*62*), we verified our atom exchange estimates calculated from the aqueous phase ^{57}Fe isotope composition by also tracking release of ^{54}Fe from the solids to the aqueous phase, since

the starting aqueous phase Fe(II) is highly depleted in ^{54}Fe. The amount of exchange estimated from the depletion of aqueous ^{57}Fe was within a few percent of that estimated from the increase of aqueous ^{54}Fe (Table 2).

Little effect of adsorbed As(V) on atom exchange between aqueous Fe(II) and magnetite was observed at high As(V) concentrations of up to 100 μM; however, some inhibition was observed at an As(V) concentration of 200 μM (Figure 8). The arsenate adsorption isotherm for magnetite indicates that at 200 μM As(V) the magnetite is slightly below surface saturation at pH 7.2 (Figure 7). At this surface coverage, the arsenate anions may inhibit direct access of Fe(II) to the surface of the magnetite, thus slowing the process of electron transfer from the aqueous Fe(II) to the mineral and decreasing the observed rate of atom exchange.

It has previously been observed that many trace elements can be incorporated into Fe oxides in the presence of Fe(II). In particular, incorporation of As(V) during the Fe(II)-catalyzed recrystallization of the unstable Fe oxides ferrihydrite and lepidocrocite to more stable Fe oxides such as goethite and magnetite has been hypothesized (*27*, *36*, *37*). To test whether As(V) would be incorporated into the stable Fe oxide magnetite in the presence of Fe(II), we used NaOH to extract the adsorbed As(V) from magnetite before reaction with Fe(II), as well as after 2 days and 18 days of reaction with Fe(II). We attribute the As(V) removed by the NaOH extraction as adsorbed and the As(V) remaining in the residual solids after extraction as incorporated.

The NaOH extraction recovered 83% of the total arsenic from magnetite before and after a 2 day reaction with 1 mM Fe(II) (Table 3). Therefore, we observed no evidence for As(V) incorporation over 2 days, despite observing almost 50% Fe atom exchange between aqueous Fe(II) and magnetite (Figure 8). However, after 18 days reaction with 1 mM Fe(II), we did observe a slight decrease in the amount of NaOH extractable As(V): 73% of the As(V) was recovered by NaOH extraction and 14% from the residual solids (Table 3). This suggests that As(V) incorporation may occur over a

longer timescale and may not be driven by Fe atom exchange alone. It has been previously observed that the rate of trace metal *release* from an iron oxide may be substantially slower than the rate of Fe atom exchange between the iron oxide and aqueous Fe(II). For example, more than 90% Fe atom exchange was observed to occur between aqueous Fe(II) and a nickel-substituted goethite over 10 days, whereas only about 6% of the total incorporated nickel was released to solution during that time span (*63*). Our research suggests that the rate of trace element *incorporation* may also be substantially slower than the rate of Fe atom exchange.

XAS analysis of As(V) adsorbed on magnetite for different lengths of time suggest that As(V) may also be incorporated into magnetite even in the absence of added Fe(II). Arsenic edge XAS spectra show that, when As(V) is adsorbed on magnetite, after a fairly short (30 minute) equilibration time, the As(V) coordination is consistent with the inner-sphere complexation of As(V) at the magnetite surface (Figure 9), similar to what has been previously observed (*36*, *64*). However, at longer adsorption times, the As-Fe coordination peak near 2.986 Å in the Fourier transform data shows a consistent increasing trend from 30 minutes, to 3.5 days, to 4 weeks of reaction time between adsorbed As(V) and magnetite. After 4 weeks, this peak is about 60% of the amplitude of the 2.986 Å peak in the XAS spectrum of an As(V)-magnetite coprecipitate (Figure 9). This observed trend suggests that over time adsorbed As(V) may become incorporated in the magnetite structure or in a secondary As-Fe phase that either remains as a layer on the magnetite particle or forms a segregated phase. Although Fe(II) has not been added to this system, it is possible that structural Fe(II) from the magnetite itself may be released into solution over time, leading to Fe(II)-catalyzed recrystallization of magnetite coupled with incorporation of As(V). Alternatively, diffusion may be responsible for the incorporation of As(V) into the magnetite structure.

XAS observations also suggest that adding Fe(II) to a magnetite-As(V) system actually inhibits As(V) incorporation when compared with an Fe(II)-free system. The

Fourier transform of the data for magnetite reacted with As(V) for 1 week in the presence of Fe(II) had similar As-Fe features to the 30 minute adsorption sample without Fe(II) (Figure 9). It is possible that added Fe(II) promotes an As-Fe(II) passivation layer that inhibits recrystallization of magnetite during the conveyor belt dissolution-reprecipitation. This interpretation is supported by the observed loss of crystallinity as observed in the suppressed amplitudes of the pXRD spectra in samples with added Fe(II) (Figure 10).

In order to investigate the influence of coprecipitated As(V) on Fe atom exchange, magnetite was precipitated in the presence of As(V), under conditions in which incorporation of As(V) into the magnetite structure is hypothesized to occur based on XAS observations (*55*). This precipitation method resulted in magnetite-As(V) precipitates with As:Fe mole ratios of 0.0005, 0.0010, and 0.0099, which fall towards the high end of the As:Fe ratios observed in naturally occurring Fe oxides, (2.4×10^{-6} to 0.09) (*7*–*9*). The significant amount of solid-associated As(V) remaining after desorption with NaOH (over 50% in all cases) suggests that some As(V) was incorporated into the magnetite structure during precipitation (Table 3), in agreement with the findings from the XAS data of Wang *et al.* (*55*). Controls with As(V) adsorbed on magnetite for less than 12 hours indicate that the NaOH extraction is able to recover 85-97% of the As(V).

To further probe the As speciation in the coprecipitation samples, we collected As edge XAS spectra. When magnetite is precipitated in the presence of As(V), a strong peak is observed near 2.986 Å in the Fourier transform data, which is higher than the peak observed in any of the adsorption samples. Fits showed an As-Fe distances of 3.44 Å for the co-precipitation sample, consistent with the observations of Wang *et al.* (*55*), so their interpretation of As substitution in the tetrahedral sites of magnetite can be applied to our co-precipitate as well. We observed highly similar As-edge spectra from the As(V)-magnetite coprecipitate before and after NaOH extractions (Figure 11), suggesting that the stable As complex is the dominant species.

We do observe a slight difference in As-Fe distances between the As(V)-magnetite coprecipitate and the short- or long-term adsorption samples: the features in the real part of the FT from the coprecipitate are at R+Δ = 2.986 Å and in the adsorption samples are at R+Δ = 2.952 Å, a difference of 0.03 Å (data not shown). This difference could be due to a less-constrained surface structure in the adsorption samples as compared with the coprecipitate. It is also possible that a distinct As-Fe phase was formed during coprecipitation. However, the distances for both the adsorption and coprecipitate Fe signals are 0.06 Å larger than the Fe signal in scorodite ($Fe^{III}AsO_4.2(H_2O)$), R+Δ = 2.889 Å, suggesting that scorodite was not formed. Scorodite formation can also be ruled out by looking at the chi(k) data (not shown). The symplesite ($Fe^{II}_3(AsO_4)_2.8(H_2O)$) spectrum looks significantly different than the data collected on the As(V) magnetite samples, ruling out symplesite formation as well (not shown). Furthermore, the XRD pattern of the As(V)-magnetite coprecipitate is similar to that of magnetite precipitated in the absence of As(V), and does not show any indication of symplesite or scorodite formation (Figure 5).

Finally, a shoulder is present in the XANES data for the As(V)-magnetite coprecipitate, which may be due to As(V) to As(III) reduction (~20% As(III)/Total As) (Figure 12). This XANES feature could also arise for structural reasons, e.g. due to incorporation of As(V) in a solid structure. For instance, there is a difference between dissolved As(V) and As(V) in scorodite. However, the features in the co-precipitate spectra in the magnetite system are outside the difference between dissolved As(V) and As(V) in scorodite, so they are likely due to reduction of As(V) to As(III). This shoulder in the XANES data was previously observed during As(V)-magnetite coprecipitation by the same method, and fitting of the shoulder suggested that a ~12-18% As(III) component was present (*36*). The authors of that study attributed the observed arsenic reduction to beam-induced reduction due to the presence of cellulose used to dilute the sample, but their measurements were done at 10 K so this explanation is unlikely. In our systems

there was no additional organic material in the sample to act as electron donor; we did not observe beam-induced evolution in our spectra, which were taken at room temperature and hence more susceptive to radiation induced chemistry; and, we did not observe As reduction in the sorption samples, suggesting that beam-induced As(V) reduction did not occur. Since the coprecipitate was prepared from a mixed Fe(II)-Fe(III) solution, it is possible that intermediate Fe(II) phases were reactive enough to reduce some As(V) to As(III) during the coprecipitation reactions. It is also possible that, in the presence of As(V), the magnetite synthesis conditions favor the formation of an unidentified $As^{III}_{0.2}$-$As^{V}_{0.8}$-Fe^{II}_{x}-Fe^{III}_{y}-O/OH_z phase (in which As(V) is more favorably reduced), with the remaining Fe(II) and Fe(III) forming magnetite.

The As(V)-magnetite coprecipitates were reacted with 1 mM Fe(II) for 7 days to investigate the influence of coprecipiated As(V) on Fe atom exchange. The presence of coprecipitated As(V) at these values corresponded with a slightly higher rate of change of ^{57}Fe enrichment in the aqueous and solid phases over time, indicating a slightly higher extent of Fe atom exchange after 7 days (Figure 8).

In addition to catalyzing the incorporation of trace elements into Fe oxides, Fe(II) has also been observed to catalyze the release of trace elements. In the presence of Fe(II), release of Ni and Zn from Ni- and Zn-substituted goethite and hematite (*40*, *42*), release of Mn from Mn-substituted goethite (*43*), and release of Co from Co-ferrite (a mineral isomorphic with magnetite, where Fe(II) is replaced by Co^{2+}) (*25*) has been observed. Under the conditions of our experiment, if any As(V) were liberated from the magnetite structure, it would be expected to immediately re-adsorb to the magnetite surface. Thus Fe(II)-catalyzed arsenic release could not be measured by tracking solution concentrations of As(V), which would be expected to remain close to zero throughout the experiment. Instead, we used NaOH extractions on the As-magnetite coprecipitate before and after reaction with 1 mM aqueous Fe(II) to determine whether As(V) would be redistributed from the magnetite structure to an adsorbed, extractable phase on the

magnetite surface over time. The results of the NaOH extractions revealed that approximately 26% of the arsenic was extractable both before and after 5 days of reaction with Fe(II) (Table 3). Therefore, we observed no evidence for As(V) redistribution to the magnetite surface after 5 days reaction with Fe(II), despite observing 75% atom exchange between aqueous Fe(II) and magnetite (Figure 8).

Effect of As(V) on Fe(II)-catalyzed recrystallization of goethite.

We also investigated the rate and extent of Fe atom exchange between aqueous Fe(II) and goethite in the presence of varying concentrations of adsorbed arsenic and with goethite co-precipitated with As(V). Consistent with our previous work (*24*), goethite in the absence of As(V) undergoes near-complete Fe atom exchange, where the fraction of ^{57}Fe ($f^{57}Fe = {}^{57}Fe/\Sigma Fe$) in the aqueous phase decreased substantially over time while the fraction in the solid phase (solids + Fe(II) taken up by the solids) increased (Figure 13 and Table 4). We again found excellent agreement between the amount of exchange estimated from the depletion of aqueous ^{57}Fe and the increase of aqueous ^{54}Fe (within a few percent; Table 4).

Goethite was then reacted with Fe(II) in the presence of 13.3 μM As(V) for 7 days to investigate the influence of adsorbed As(V) on Fe atom exchange. At this arsenic loading and circumneutral pH, near-complete adsorption of the As(V) is observed (Figure 7), which is consistent with previous observations of significant As(V) adsorption on goethite at circumneutral pH (*65*). The presence of adsorbed As(V) at this concentration showed little effect on the change in ^{57}Fe in the aqueous and solid phases over time, indicating negligible influence on the extent of Fe atom exchange. At high As(V) concentrations (100 – 267 μM), however, we measured significant inhibition of Fe atom exchange (Figure 14). The arsenic adsorption isotherm for the nanogoethite indicates that at 267 μM As(V) the goethite is slightly below surface saturation at pH 7.5 (Figure 7).

Similar to what we observed with magnetite, the adsorbed arsenate anions may inhibit direct access of Fe(II) to the surface of the goethite, thus slowing the process of electron transfer from the aqueous Fe(II) to the mineral and decreasing the observed rate of atom exchange.

We additionally observed Fe atom exchange under conditions in which Catalano *et al.*(*50*) observed no incorporation of As(V) into goethite (dashed line in Figure 14). Under these conditions (i.e. a higher solids loading, decreased pH, and larger goethite particle size), we observed approximately 40% atom exchange over 7 days, compared to approximately 80% under our group's experimental conditions for an adsorbed As(V) concentration of 100 μM (Figure 14).

To test whether As(V) would be incorporated into goethite in the presence of Fe(II) under experimental conditions that result in higher atom exchange than the Catalano group's conditions, we used NaOH to extract the adsorbed As(V) from nanogoethite before and after 3 days of reaction with Fe(II) and 13.3 μM As(V) at pH 7.5. We observed no evidence for As(V) incorporation (Table 3), despite observing more than 80% Fe atom exchange between aqueous Fe(II) and goethite (Figure 14). However, as noted above, As(V) incorporation into magnetite is observed to occur on a much longer timescale than atom exchange; therefore, longer reaction times will be required to determine whether As(V) can be incorporated into goethite in the presence of Fe(II).

In contrast with our observations for magnetite, XAS spectra of As(V) adsorbed on goethite in the absence of Fe(II) do not indicate incorporation of As(V) over time. After both a 10 minute and a four day adsorption time, the As(V) coordination is consistent with the inner-sphere complexation of As(V) at the goethite surface (Figure 15), similar to what has been previously observed for As(V) adsorption on goethite (*50*, *66*, *67*).

In order to investigate the influence of coprecipitated As(V) on Fe atom exchange, goethite was precipitated in the presence of As(V), under conditions in which

incorporation of As(V) into the goethite structure is hypothesized to occur based on chemical extraction data (*68*). This method produced poorly crystalline nanogoethite, which demonstrated even more rapid atom exchange than our more crystalline nanogoethite (Figure 16). The coprecipitation resulted in goethite-As(V) precipitates with As:Fe mole ratios of 0.0008, 0.0015, and 0.0155, which fall towards the high end of the As:Fe ratios observed in naturally occurring Fe oxides (2.4×10^{-6} to 0.09) (*7–9*). The significant amount of solid-associated As(V) remaining after desorption with NaOH (over 40% in all cases) suggests that some As(V) was incorporated into the goethite structure during precipitation (Table 3), in agreement with the chemical extraction data of Pedersen *et al.* (*68*). Controls with As(V) adsorbed on goethite indicate that the NaOH extraction is able to recover 87-88% of the As(V).

To further probe the As speciation in the coprecipitation samples, we collected As edge XAS spectra. Slight differences exist between the spectra of As(V) co-precipitated with goethite and As(V) reacted with pre-formed goethite (Figure 15). Analysis of the co-precipitate sample spectrum indicates the same As-Fe amplitudes and distances as in the adsorption samples, but a suppressed amplitude in the As-O signal suggests a disordered AsO_4 tetrahedron. It is possible that the internalization of the AsO_4 tetrahedron in a crystal cavity occurs in the co-precipitation sample, with the inner-sphere binding mechanism to the neighboring Fe octahedra remaining the same as in the adsorption samples.

Finally, a shoulder is present in the XANES data for the As(V)-goethite coprecipitate, which may be due to As(V) to As(III) reduction (~5% As(III)/Total As) (Figure 17). Since the coprecipitate was prepared by oxidizing a Fe(II) solution, it is possible that intermediate Fe(II) phases were reactive enough to reduce some As(V) to As(III) during the coprecipitation reactions. However, the XANES feature could also arise for structural reasons, for example, due to incorporation of As(V) in a solid structure. The features in the co-precipitate spectra are within the difference between dissolved As(V) and As(V) in

scorodite, so we cannot address whether the spectral differences are due to valence state or structure.

The As(V)-goethite coprecipitates were reacted with 1 mM Fe(II) for 7 days to investigate the influence of coprecipiated As(V) on Fe atom exchange. The presence of coprecipitated As(V) at these values showed little effect on the change in ^{57}Fe in the aqueous and solid phases over time, indicating negligible influence on the extent of Fe atom exchange (Figure 16; Table 4).

Effect of As(V) on Fe(II)-catalyzed recrystallization of ferrihydrite.

We investigated the rate and extent of Fe atom exchange during the Fe(II)-catalyzed transformation of 2-line ferrihydrite at varying concentrations of Fe(II). It has been suggested based on kinetic data on 6-line ferrihydrite transformation that ferrihydrite transforms to goethite and minor amounts of magnetite via a dissolution-reprecipitation mechanism at low Fe(II) concentrations ($\leq$ 0.36 mM), and that ferrihydrite transforms to magnetite via a solid-state transformation mechanism at high Fe(II) concentrations ($\geq$ 1.8 mM) (*69*). Here, we investigate the mechanism of ferrihydrite transformation by tracking Fe atom exchange. Complete atom exchange between aqueous Fe(II) and Fe oxide during transformation is consistent with a dissolution-reprecipitation transformation mechanism in which all Fe atoms from the iron oxide are released into solution before reprecipitating as a new Fe oxide. In contrast, little-to-no atom exchange during transformation is consistent with a solid-state transformation mechanism in which there is little-to-no release of Fe atoms from the Fe oxide into solution during transformation.

The observed extent of Fe atom exchange has varied in previous studies of Fe oxide transformation. For example, complete atom exchange between a ^{55}Fe-labeled Fe oxide and an Fe(II) spike of natural isotopic composition was observed during the

transformation of ferrihydrite to lepidocrocite (0.2 mM Fe(II)) and goethite (1 mM Fe(II)) (*28*) and during the transformation of an As(V)-ferrihydrite coprecipitate to lepidocrocite/goethite (0.2 mM Fe(II)) and goethite/magnetite (1 mM Fe(II)) (*68*), consistent with a dissolution-reprecipitation mechanism for these transformations. Complete atom exchange was also observed during the transformation of lepidocrocite and an As(V)-lepidocrocite coprecipitate to magnetite (1 mM Fe(II)); however, very little atom exchange was observed during the transformation of two additional As(V)-lepidocrocite coprecipitates to magnetite (1 mM Fe(II)) (*68*). These data suggest that whether transformation occurs via a dissolution-reprecipitation or a solid-state mechanism may be affected by the As:Fe ratio in the coprecipitate as well as by minor variations in mineral synthesis conditions.

We investigated the rate and extent of Fe atom exchange between aqueous Fe(II) and Fe oxide during the Fe(II)-catalyzed transformation of 2-line ferrihydrite at low (0.2 mM) and high (5 mM) concentrations of Fe(II). At a low (0.2 mM) Fe(II) concentration we observed conversion of ferrihydrite to lepidocrocite, and at a high (5 mM) Fe(II) concentration we observed conversion of ferrihydrite to lepidocrocite and then to magnetite during a 5-day reaction (Figure 18). Complete atom exchange was observed after 2 days for both Fe(II) concentrations (Figure 19; Table 5). Our observation of complete atom exchange at a 0.2 mM Fe(II) concentration is consistent with previous experimental observations of ferrihydrite transformation to a goethite/lepidocrocite or goethite/magnetite assemblage via dissolution-reprecipitation at Fe(II) concentrations of 1 mM or less (*28*, *52*, *70*). However, our observation of complete atom exchange for the transformation of ferrihydrite to magnetite at a concentration of 5 mM Fe(II) over the course of 5 days contradicts the kinetics-based hypothesis of Yang *et al.* (*69*) which suggests that this transformation occurs via a solid-state mechanism.

In order to determine the effects of adsorbed As(V) on the mechanism and kinetics of ferrihydrite transformation, we tracked Fe atom exchange during ferrihydrite

transformation in the presence of 206 μM As(V) and 5 mM Fe(II). At this concentration, As(V) slowed the rate of Fe atom exchange between aqueous Fe(II) and ferrihydrite (Figure 19). Complete atom exchange was only observed after 22 days of reaction in the presence of 206 μM As(V), in contrast with 2 days of reaction in the absence of As(V). This is similar to our observed inhibitory effect of As(V) on atom exchange between Fe(II) and goethite and magnetite, which suggests that inhibition of atom exchange may occur by the same mechanism. The presence of adsorbed As(V) also slowed the transformation of ferrihydrite to more stable iron minerals (Figure 18), which is consistent with previous observations (*71*, *72*). However, the degree of Fe atom exchange did not directly correlate with the amount of ferrihydrite transformed, since over 70% atom exchange occurred before any mineral transformation was observed. Adsorbed Si and natural organic matter have similarly been observed to decrease the rate of Fe atom exchange and mineral transformation of the Fe(III) minerals ferrihydrite, jarosite, lepidocrocite, and schwertmannite, and a similar lack of correlation between Fe atom exchange and mineral transformation was observed under those conditions (*26*).

Environmental Implications

The observation that high concentrations of As(V) inhibit the Fe(II)-catalyzed recrystallization of the Fe oxides goethite, magnetite, and ferrihydrite has implications for contaminant fate and transport in the environment. For example, inhibition of recrystallization by adsorbed As(V) may result in a lower release of trace elements present in the Fe oxide structure compared with what would otherwise occur in the absence of As(V). However, inhibition of recrystallization by adsorbed As(V) might also decrease the rate of uptake and sequestration of contaminants from groundwater into the Fe oxide structure.

The observation that As(V) may be incorporated into magnetite over long time periods both in the presence and absence of aqueous Fe(II) also has implications for

arsenic mobility in the environment. Further research should be done to determine whether As(V) is incorporated into goethite in the presence of Fe(II) on long timescales, whether As(V) is released from As(V)-magnetite or As(V)-goethite coprecipitates on long timescales, and whether As(V) is incorporated into transformation products during the Fe(II)-catalyzed transformation of ferrihydrite.

Table 1 Properties of iron oxides used in this study (± 1 standard deviation, when given).

Sample ID	Synthesis Parameters				Solid properties			
	As:Fe mole ratio	pH	Temp. (°C)	Aging Time (day)	As:Fe mole ratio[a]	BET Surface area (m^2/g)	Stoichiometry (*x*)	Identity Confirmed by XRD?
				Goethite				
Microgoethite[b]	0	0.3 M KOH	70	2.5	n.m.[c]	36.39 ± 1.65[d]	NA	Y
Nanogoethite[e]	0	12	90	1	n.m.	116.93[f]	NA	Y
Poorly Crystalline Goethite	0	7	Room temp.	1	n.m.	n.m.	NA	Y
As(V)-Goethite Coprecipitate (0.0008)	0.0010	7	Room temp.	1	0.0008 ± 0.00001[g]	n.m.	NA	Y
As(V)-Goethite Coprecipitate (0.00153)	0.0010	7	Room temp.	1	0.00153 ± 0.00013[g]	n.m.	NA	Y
As(V)-Goethite Coprecipitate (0.0155)	0.0100	7	Room temp.	1	0.0155 ± 0.00017[g]	n.m.	NA	Y
				Magnetite				
Magnetite	0	10-11	Room temp.	1	n.m.	65.30[f]	0.45 ± 0.02[h]	Y
As(V)-Magnetite Coprecipitate (0.0005)	0.0011	10-11	Room temp.	1	0.0005 ± 0.00001[i]	n.m.	0.49 ± 0.04[h]	N
As(V)-Magnetite Coprecipitate (0.0010)	0.0010	10-11	Room temp.	1	n.m.	n.m.	n.m.	N
As(V)-Magnetite Coprecipitate (0.0099)	0.0100	10-11	Room temp.	1	0.0099 ± 0.00153[h]	n.m.	0.50 ± 0.03[h]	Y
				Ferrihydrite				
Ferrihydrite	0	8	Room temp.	0	n.m.	325.85[f]	NA	Y

[a] = As:Fe mole ratio determined by dissolution in HCl. As(V) concentration was measured on ICP-MS and Fe concentration was measured spectrophotometrically by the phenanthroline method.

[b] = Used for Fe atom exchange experiments between Fe(II) and goethite with 100 µM adsorbed As(V) at conditions analogous to those of Catalano et al. (*50*).

[c] = Not measured.

[d] = Mean and one standard deviation of triplicate BET measurements.

[e] = Used for Fe atom exchange experiments between Fe(II) and goethite with 0, 13.3, 100, and 267 µM adsorbed As(V); Fe(II)-catalyzed goethite recrystallization experiment followed by As extractions.

[f] = Single BET measurement.

[g] = Mean and one standard deviation of triplicate reactors of 30 mg goethite dissolved in concentrated HCl.

Table 1 – continued

[h] = Mean and one standard deviation of triplicate reactors of 15 mg magnetite dissolved in 5 M HCl.

[i] = Mean and one standard deviation of triplicate reactors of 10 mg magnetite dissolved in 5 M HCl.

Table 2 Effect of coprecipitated and adsorbed As(V) on rates of Fe(II)-catalyzed Fe atom exchange of 1 gL^{-1} magnetite in 50 mM MOPS at pH 7.2.

		Aqueous Fe(II)					Residual Solid						
	Time (day)	Fe(II) (umol)	% ^{57}Fe	% ^{54}Fe	% Ex. (^{57}Fe)	% Ex. (^{54}Fe)	Fe (umol)	% ^{57}Fe	% ^{54}Fe	% Ex. (^{57}Fe)	% Ex. (^{54}Fe)	% Fe Recovery	pH
No As(V)	0	14.5 (0.2)	90.4 (1)	0.5 (0.05)	0 (1.3)	0 (1.1)	213 (22.5)	2.4 (0.1)	5.1 (0.06)	0 (0.8)	0 (1.6)	108.9 (10.9)	---
	0.01	14.5 (0.3)	62.6 (11.3)	1.9 (0.56)	34.1 (13.8)	32.9 (13.1)	183.6 (53.5)	4.6 (0.4)	4.9 (0.11)	35.7 (7)	56.2 (3.1)	94.8 (25.8)	7.27 (0.03)
	4.78	12.7 (0.4)	40.3 (5.3)	3 (0.24)	61.4 (6.5)	58.4 (5.7)	203.5 (30.6)	6.6 (0.1)	4.7 (0.09)	66.3 (2)	105.7 (2.5)	103.5 (14.5)	7.15 (0.05)
	6.91	12.7 (1.5)	42.7 (5.5)	2.9 (0.31)	58.5 (6.7)	56.8 (7.4)	228 (27)	6.5 (0.3)	4.7 (0)	66 (5.4)	102.6 (0.1)	115.2 (12.4)	7.16 (0.04)
As(V) Ads 13.3 µM	0	14.2 (0.4)	82.7 (1.9)	1.1 (0.07)	0 (2.5)	0 (1)	213 (22.5)	2.4 (0.1)	5.1 (0.06)	0 (0.9)	0 (1.9)	108.8 (10.9)	---
	0.01	19.6 (2.9)	46.9 (6.8)	2.8 (0.3)	48 (9.1)	46.1 (4.2)	177.5 (3.2)	4.6 (0.2)	5.1 (0.08)	39.4 (3.3)	-6.2 (2.5)	94.4 (0.5)	7.14 (0.11)
	4.77	15.3 (0.5)	40.2 (2.2)	3.1 (0.1)	57 (3)	55.8 (1.4)	187 (2.2)	6.3 (0.4)	4.8 (0.16)	67.6 (6.5)	81.2 (5.3)	96.9 (1.2)	7.17 (0.02)
	6.91	14.8 (0.3)	37.1 (1.7)	3.3 (0.06)	61.2 (2.3)	60.4 (0.9)	183.4 (9)	6.9 (0)	4.9 (0.03)	78.1 (0.1)	49 (1.1)	94.9 (4.4)	7.17 (0.05)
As(V) Ads 100 µM	0	14.6 (0.4)	90.8 (1)	0.3 (0)	0 (1.3)	0 (0.5)	213 (22.5)	5.1 (0.1)	0 (0.8)	0 (0.8)	0 (1.6)	109 (10.8)	NA
	0.01	14.5 (0.3)	67 (3)	1.6 (0.2)	29 (3.6)	29.1 (2.1)	193.8 (12)	3.9 (0)	24.7 (0.4)	24.7 (0.4)	78.7 (1.5)	99.7 (5.7)	7.25 (0.01)
	4.77	14.2 (0.3)	47.2 (6.5)	2.6 (0.4)	53.2 (7.9)	51.7 (4.8)	187.3 (7.9)	5.6 (0.1)	51.4 (1.1)	51.4 (1.1)	104.3 (1.2)	96.5 (3.7)	7.17 (0.01)
	6.95	13.4 (0.5)	46.2 (5.7)	2.6 (0.3)	54.3 (6.9)	52.1 (3.4)	185.1 (30.3)	5.4 (0.2)	48.4 (3.9)	48.4 (3.9)	106.2 (0.4)	95.1 (14.5)	7.18 (0.02)

Table 2 – continued

	Time (day)	Aqueous Fe(II)					Residual Solid					% Fe Recovery	pH
		Fe(II) (umol)	% ^{57}Fe	% ^{54}Fe	% Ex. (^{57}Fe)	% Ex. (^{54}Fe)	Fe (umol)	% ^{57}Fe	% ^{54}Fe	% Ex. (^{57}Fe)	% Ex. (^{54}Fe)		
As(V) Ads 200 µM	0	17 (1.6)	87.3 (2)	0.5 (0.1)	0 (2.5)	0 (0.9)	213 (22.5)	5.1 (0.1)	0 (0.9)	0 (0.9)	0 (1.7)	110.1 (11.5)	NA
	0.01	14.2 (0.1)	70 (3.9)	1.5 (0.2)	21.9 (5)	22.5 (2.5)	209.8 (8.7)	3.7 (0)	22.3 (0.1)	22.3 (0.1)	98.6 (0.7)	107.3 (4.2)	7.17 (0.01)
	5.04	13 (0.2)	60.6 (1.6)	1.9 (0.1)	33.9 (2.1)	33.3 (1.7)	177.4 (10.8)	5.2 (0.4)	45.5 (6.7)	45.5 (6.7)	116.2 (1.1)	91.1 (5.3)	7.14 (0.02)
	6.82	12.6 (0.2)	57.4 (3.1)	2.1 (0.2)	37.9 (4)	37.5 (2.1)	191 (13.8)	5.3 (0.1)	47.5 (1.9)	47.5 (1.9)	114.1 (0.9)	97.5 (6.5)	7.16 (0.02)
As(V) Coppt As:Fe = 0.0005	0	15.6 (0.2)	76 (7.1)	1.2 (0.34)	0 (10.4)	0 (5.2)	190.4 (16.4)	2.4 (0)	4.9 (0.01)	0 (0.3)	0 (0.4)	98.4 (7.7)	---
	0.01	18.7 (0.4)	32.1	3.4	64.2	63.7	196.9 (15.5)	6.7 (0)	4.7 (0.03)	82.1 (0.8)	79.2 (1)	103.1 (7.2)	7.16 (0.02)
	5.33	12.6 (0.6)	27.1 (2.4)	3.6 (0.12)	71.6 (3.5)	71.1 (1.9)	188.5 (1.7)	8.7 (0.6)	4.6 (0.02)	120.8 (10.9)	115.6 (0.9)	96.1 (1)	7.14 (0.03)
	7.82	13.1 (0.5)	28.8 (2.7)	3.6 (0.14)	69.1 (3.9)	68.9 (2.2)	176.5 (2.5)	9 (0.1)	4.6 (0.05)	125.8 (1.8)	131.3 (1.7)	90.6 (1.4)	7.1 (0.01)
As(V) Coppt As:Fe = 0.0099	0	15.8 (0.2)	94.1 (1.1)	0.2 (0.1)	0 (1.3)	0 (0.6)	183 (40.9)	4.8 (0)	0 (0.3)	0 (0.3)	0 (0.7)	95 (19.6)	---
	0.01	13.5 (0.9)	75.3 (2.2)	1.2 (0.1)	22 (2.6)	23.2 (1.3)	183.2 (15.4)	4.9 (0)	41.2 (0.5)	41.2 (0.5)	39.8 (1)	94 (6.9)	7.16 (0.03)
	5.07	5.3 (0.3)	30 (2.8)	3.5 (0.2)	75.1 (3.2)	76.8 (1.8)	182.7 (32.1)	9 (0.5)	104.2 (7.1)	104.2 (7.1)	99.1 (1.7)	89.8 (15.3)	7.04 (0.01)
	6.97	5.1 (0.2)	32.1 (5.5)	3.4 (0.3)	72.7 (6.4)	74.4 (3)	165.8 (32.4)	9.7 (0.9)	114.2 (13.2)	114.2 (13.2)	104.3 (1)	81.7 (15.4)	7.03 (0.01)

Table 3 NaOH extractions of As(V) from magnetite and goethite following adsorption, coprecipitation, and Fe(II)-catalyzed mineral recrystallization.

		Initial added	Aqueous		NaOH extraction *"adsorbed"*		Residual solids *"incorporated"*		Total recovery	
		nmol	nmol	%	nmol	%	nmol	%	nmol	%
Magnetite										
	Adsorbed As(V) + Fe(II)									
As(V) concentration = 13.3 µM	t = 0 d	200	8*(15)*	4*(7)*	165*(12)*	83*(6)*	5*(1)*	3*(0)*	182*(2)*	91*(1)*
	t = 2 d	200	0*(0)*	0*(0)*	165*(5)*	83*(2)*	7*(1)*	4*(1)*	79*(4)*	89*(2)*
	t = 18 d	200	0(0)	0(0)	146(6)	73(3)	7(4)	14(2)	73(8)	87(4)
	As(V) Coprecipitates									
As:Fe mole ratio = 0.0005	Coprecipitate	64	---	---	18*(2)*	29*(3)*	44*(5)*	68*(9)*	64*(7)*	99*(12)*
	Adsorption Control	98	0*(0)*	0*(0)*	95*(11)*	97*(11)*	3*(1)*	4*(1)*	98*(12)*	100*(12)*
0.0010	Coprecipitate	200	18*(27)*	1*(2)*	54*(7)*	39*(18)*	102*(21)*	51*(11)*	176*(5)*	88*(3)*
	Adsorption Control	200	0*(0)*	0*(0)*	184*(9)*	85*(4)*	17*(1)*	9*(0)*	191*(8)*	95*(4)*
0.0099	Coprecipitate	2055	---	---	524*(116)*	26*(6)*	1318*(253)*	64*(12)*	1842*(368)*	90*(18)*
	Coprecipitate + Fe(II) t = 5 d	2055	0*(0)*	0*(0)*	538*(63)*	26*(3)*	1375*(67)*	67*(3)*	1914*(88)*	96*(5)*
	Adsorption Control	1912	31*(28)*	2*(1)*	1778*(39)*	93*(1)*	100*(2)*	5*(0)*	1909*(12)*	100*(1)*

Table 3 – continued

		Initial added	Aqueous		NaOH extraction *"adsorbed"*		Residual solids *"incorporated"*		Total recovery	
		nmol	nmol	%	nmol	%	nmol	%	nmol	%
Goethite										
	Adsorbed As(V) + Fe(II)									
As(V) concentration = 13.3 µM	t = 0 d	200	0*(0)*	0*(0)*	176*(4)*	88*(2)*	3*(0)*	2*(0)*	184*(0)*	92*(0)*
	t = 3 d	200	0*(0)*	0*(0)*	179*(4)*	89*(2)*	5*(0)*	2*(0)*	187*(6)*	93*(3)*
	As(V) Coprecipitates									
As:Fe mole ratio = 0.0008	Coprecipitate	261	---	---	156*(4)*	60*(1)*	117*(4)*	45*(2)*	273*(8)*	105*(3)*
	Adsorption Control	277	0*(0)*	0*(0)*	239*(41)*	87*(15)*	39*(23)*	14*(8)*	279*(59)*	101*(22)*
0.0015	Coprecipitate	250	---	---	142*(25)*	57*(10)*	145*(10)*	58*(4)*	287*(20)*	115*(8)*
0.0155	Coprecipitate	5258	---	---	2862*(140)*	54*(3)*	2126*(130)*	40*(2)*	4988*(222)*	95*(4)*

Table 4 Effect of coprecipitated and adsorbed As(V) on rates of Fe(II)-catalyzed Fe atom exchange of 2 gL^{-1} goethite in 25 mM HEPES/25 mM KBr at pH 7.5.

		Aqueous Fe(II)					Residual Solid						
	Time (day)	Fe(II) (umol)	% ^{57}Fe	% ^{54}Fe	% Ex. (^{57}Fe)	% Ex. (^{54}Fe)	Fe (umol)	% ^{57}Fe	% ^{54}Fe	% Ex. (^{57}Fe)	% Ex. (^{54}Fe)	% Fe Recovery	pH
No As(V)	0	14.5 (0.2)	83 (6)	1 (0.3)	0 (7.8)	0 (5.9)	349 (10.2)	2 (0.1)	4.8 (0.01)	0 (1.8)	0 (5.6)	102.9 (2.84)	---
	0.0069	4.5 (0.1)	60.4 (1.5)	2 (0.05)	29 (2)	29 (1.1)	339 (21.8)	5 (0)	4.6 (0.05)	78.3 (1.3)	120.9 (29.7)	97.2 (6.15)	---
	3	3.5	14.8	4	88	87	329	6.2	4.6	113.7	122.7	94	---
	7	3.5	11.5	4	93	91	334	6.2	4.6	111.6	116.6	95.5	---
As(V) Ads 13.3 uM	0	16.4	88.7	0.5	0	0	349.3 (10.2)	2.3 (0.1)	4.8 (0.01)	0 (1.7)	0 (5.3)	103.3	---
	0.0069	6.9 (0.6)	80.6 (7.2)	0.9 (0.3)	9.7 (8.7)	9.5 (6.2)	353.4 (67.6)	4.7 (0.2)	4.7 (0.02)	65.1 (5.4)	42.2 (12.1)	101.7 (18.9)	---
	3	7.2 (2.6)	21 (2)	3.8 (0.1)	81.8 (2.4)	79.2 (0.1)	320.8 (7)	6.8 (0.2)	4.6 (0.02)	121.8 (4.3)	94.4 (12.1)	91.6 (1.3)	---
	7	8.6	16.9	4	86.9	84.9	338.3	7.1	4.6	128.9	113.6	98	---
As(V) Ads 100 uM	0	14.9 (0.2)	80.7 (5)	0.9 (0.27)	0 (6.7)	0 (7)	333.4 (5.4)	2.4 (0)	5 (0.03)	0 (0.5)	0 (0.5)	98.8 (1.5)	---
	0.006944	6.4 (0.2)	73.9 (2)	1.3 (0.09)	9.1 (2.7)	9.5 (2.2)	341.4 (25.8)	5.1 (0)	4.8 (0.04)	80.9 (1.1)	80.9 (1.1)	98.6 (7.4)	7.45 (0.03)
	2.95	7 (0.2)	28.7 (1.2)	3.6 (0.07)	69.3 (1.6)	69 (1.7)	319.7 (11.3)	6.2 (0.1)	4.8 (0.04)	113.8 (2)	113.8 (2)	92.7 (3.2)	7.43 (0.02)
	6.815972	6.5 (0.3)	22.2 (1.3)	3.9 (0.12)	78 (1.8)	77.5 (3)	325.4 (3.9)	6.3 (0.1)	4.8 (0.01)	117.6 (1.9)	117.6 (1.9)	94.1 (1.1)	---

Table 4 – continued

	Time (day)	Aqueous Fe(II)					Residual Solid					% Fe Recovery	pH
		Fe(II) (umol)	% ^{57}Fe	% ^{54}Fe	% Ex. (^{57}Fe)	% Ex. (^{54}Fe)	Fe (umol)	% ^{57}Fe	% ^{54}Fe	% Ex. (^{57}Fe)	% Ex. (^{54}Fe)		
Catalano As(V) Ads 100 uM	0	15 (0.3)	92.7 (0.2)	0.4 (0.01)	0 (0.3)	0 (0.2)	622.8 (38.8)	2.4 (0)	4.9 (0.1)	0 (1.9)	0 (88.3)	92.4 (5.6)	---
	0.006944	11.3 (0.3)	88 (0.9)	0.6 (0.05)	5.3 (1.1)	5 (1.1)	592.6 (12.9)	3 (0)	4.8 (0)	33.7 (0.8)	85.8 (17.9)	87.5 (1.9)	6.08 (0.03)
	4.96875	11.1 (0.3)	59.9 (5.4)	2.1 (0.32)	37.1 (6.2)	38.6 (7.1)	592.8 (7.5)	3.6 (0)	4.8 (0)	63.6 (1.6)	87.5 (3.3)	87.5 (1.1)	5.93 (0.07)
	6.885417	11.1 (0.1)	57.9 (4.3)	2.1 (0.22)	39.4 (4.8)	40.2 (5)	---	---	---	---	---	---	5.92 (0.06)
As(V) Ads 267 uM	0	15.4 (0.5)	87 (2.9)	0.6 (0.15)	0 (3.6)	0 (2.9)	349.3 (10.2)	---	---	---	---	103 (3)	---
	0.008333	9.6 (0.3)	83.6 (2.1)	0.8 (0.08)	4.2 (2.6)	4.6 (1.6)	354.1 (56.4)	---	---	---	---	102.7 (16)	7.42 (0.03)
	4.755556	6.4 (0.9)	74.4 (1.9)	1.2 (0.08)	15.6 (2.3)	16.2 (1.6)	341.3 (25.9)	---	---	---	---	98.2 (7.6)	7.51 (0.09)
	7.993056	6.7 (0.7)	72.2 (2.6)	1.4 (0.14)	18.3 (3.3)	19.5 (2.6)	352.9 (33.6)	---	---	---	---	101.6 (9.7)	7.47 (0.05)
Poorly Crystalline Goethite No As(V)	0	15.6 (0.2)	72.8 (2.4)	1.3 (0.12)	0 (3.6)	0 (3.6)	322.9 (8.9)	2.2 (0)	4.8 (0.04)	0 (0.2)	0 (0.2)	96 (2.5)	NA
	0.006944	6.3 (0.4)	11.2 (2.1)	4.4 (0.17)	91.1 (3.1)	92.9 (5.1)	368.3 (34.5)	6.2 (0.1)	4.6 (0.05)	133.3 (4.5)	133.3 (4.5)	106.2 (9.7)	6.47 (0.03)
	2.888889	5.1 (0.7)	5 (0.7)	4.5 (0.28)	100.3 (1)	97.5 (8.2)	312 (5)	6.1 (0.6)	4.6 (0.03)	131.7 (18.7)	131.7 (18.7)	89.9 (1.3)	6.43 (0.02)
	7.927083	4.3 (0.1)	4.8 (0.5)	4.8 (0.09)	100.5 (0.7)	103.7 (2.6)	318 (7)	6.2 (0.6)	4.6 (0.1)	134.6 (21.3)	134.6 (21.3)	91 (2)	6.42 (0.01)

Table 4 – continued

	Time (day)	Aqueous Fe(II)					Residual Solid					% Fe Recovery	pH
		Fe(II) (umol)	% ^{57}Fe	% ^{54}Fe	% Ex. (^{57}Fe)	% Ex. (^{54}Fe)	Fe (umol)	% ^{57}Fe	% ^{54}Fe	% Ex. (^{57}Fe)	% Ex. (^{54}Fe)		
As(V) Coppt As:Fe = 0.0015	0	6.9 (0.4)	92 (0.1)	0.3	0 (0.1)	0	146.7 (11.2)	2.1 (0)	4.9 (0.05)	0 (0.4)	0 (0.4)	87.1 (6.1)	NA
	0.006944	2.8 (0.1)	46.1 (4.1)	2.7 (0.2)	53.5 (4.8)	55.1 (4.5)	148.3 (8.4)	5.7 (0.1)	4.7 (0.02)	92.6 (3.7)	92.6 (3.7)	85.6 (4.8)	6.39 (0.02)
	2.866667	0.9 (0.2)	6.8 (0)	4.7 (0.05)	99 (0)	100.2 (1.2)	135.9 (16.9)	6.5 (0.1)	4.6 (0.02)	112 (1.5)	112 (1.5)	77.5 (9.6)	6.53 (0.01)
	6.636111	1.1 (0.1)	6.4 (0.2)	4.7 (0.06)	99.5 (0.2)	101.3 (1.3)	156.9 (3.2)	6.3 (0.2)	4.6 (0.04)	107 (3.9)	107 (3.9)	89.6 (1.8)	6.55 (0.01)
As(V) Coppt As:Fe = 0.0155	0	6.8 (0.1)	89.7 (3)	0.4 (0.12)	0.4 (3.5)	0 (3.2)	159 (2)	2.1 (0)	4.3 (0.01)	0.1 (0.3)	0.1 (0.3)	94 (1.1)	NA
	0.006944	2.2 (0.2)	51 (10.9)	2.1 (0.45)	46.4 (13)	46.8 (11.9)	140.8 (19)	5.5 (0)	4.1 (0.02)	87.3 (1.3)	87.3 (1.3)	81 (10.8)	6.46 (0.01)
	2.938889	0.7 (0.1)	11.1 (0.3)	4 (0.07)	93.9 (0.4)	96.1 (1.7)	151.6 (5.8)	6.3 (0)	4.1 (0.03)	108.8 (1.2)	108.8 (1.2)	86.3 (3.3)	6.4 (0.03)
	6.96875	0.7 (0.1)	9.1 (0.4)	4 (0.04)	96.2 (0.5)	97.4 (1)	153.8 (8.5)	6.3 (0.1)	4.1 (0.03)	110 (2.8)	110 (2.8)	87.6 (4.9)	6.43 (0.01)

Table 5 Effect of Fe(II) concentration and arsenate on rates of Fe(II)-catalyzed Fe atom exchange of 1 gL^{-1} ferrihydrite in 50 mM MOPS at an initial pH of 7.2.

		Aqueous Fe(II)					Residual Solid						
	Time (day)	Fe(II) (umol)	% ^{57}Fe	% ^{54}Fe	% Ex. ^{57}Fe	% Ex. ^{54}Fe	Fe (umol)	% ^{57}Fe	% ^{54}Fe	% Ex. ^{57}Fe	% Ex. ^{54}Fe	% Fe Recovery	pH
0.2 mM Fe(II)	0	3.3 (0)	91.1 (1.2)	0.4 (0.1)	0 (1.4)	0 (1.7)	103.1 (3.7)	2.3 (0)	4.8 (0.1)	0 (2.3)	0 (156.5)	100.2 (3.6)	---
	0.04	0.9 (0)	33 (2.5)	3.4 (0.1)	66.8 (2.9)	69.3 (2.5)	100.9 (5.8)	4.1 (0.1)	4.8 (0)	101.8 (4.8)	-61.7 (56.7)	96.6 (5.5)	7.1 (0.02)
	2.28	0.3 (0)	4.5 (0.3)	4.8 (0)	99.4 (0.4)	101.9 (1.2)	96.6 (2)	4.3 (0)	4.8 (0)	113.5 (0.5)	25.4 (41.3)	92.2 (1.9)	7.11 (0.03)
	5.15	0.3 (0)	5.4 (2.4)	4.8 (0.2)	98.5 (2.7)	102.5 (4.6)	95.4 (6.1)	4.2 (0)	4.8 (0.1)	108.9 (1.6)	-6.4 (89.2)	90.9 (5.8)	7.1 (0.02)
5 mM Fe(II)	0	75.5 (0.2)	92.1 (2.7)	0.3 (0.1)	0 (4.5)	0 (0.4)	103.1 (3.7)	2.3 (0)	4.8 (0.1)	0 (0.1)	0 (8.9)	100.2 (2.3)	---
	0.04	57.8 (5.7)	76.6 (2)	1.1 (0.1)	25.7 (3.3)	25.8 (0.3)	106.8 (4.8)	20 (1.5)	4 (0.1)	60.3 (5.2)	53.9 (4.7)	94.9 (2.9)	7.09 (0.1)
	2.28	18.9 (4.3)	30.3 (2.1)	3.4 (0.1)	102.3 (3.5)	103.5 (0.4)	136 (7.9)	34.8 (2.5)	3.2 (0.1)	110.7 (8.5)	109.1 (5.3)	97 (3.4)	6.87 (0.05)
	5.15	13.4 (2.2)	27.5 (0.9)	3.6 (0)	106.8 (1.5)	109 (0.1)	129.1 (6.4)	34.4 (2.6)	3.2 (0.1)	109.5 (8.8)	108.8 (8.9)	90.2 (5.1)	6.84 (0.06)

Table 5 – continued

		Aqueous Fe(II)					Residual Solid						
	Time (day)	Fe(II) (umol)	% ^{57}Fe	% ^{54}Fe	% Ex. ^{57}Fe	% Ex. ^{54}Fe	Fe (umol)	% ^{57}Fe	% ^{54}Fe	% Ex. ^{57}Fe	% Ex. ^{54}Fe	% Fe Recovery	pH
5 mM Fe(II) + 206 µM As(V)	0	74.1 (2.4)	93.3 (1.1)	0.1 (0)	0 (1.8)	0 (0.1)	103.1 (3.7)	2.3 (0)	4.8 (0.1)	0 (0.1)	0 (8.6)	99.6 (3.9)	NA
	0.04	59.4 (0.1)	87.9 (4.1)	0.5 (0.2)	9 (6.6)	10.2 (0.7)	105.7 (7.3)	10.8 (0.1)	4.3 (0)	28.4 (0.2)	28.8 (1.3)	94.9 (4.7)	7.2 (0.04)
	2.07	49.8 (1.5)	68.3 (0.4)	1.4 (0)	40.8 (0.7)	41.2 (0.1)	103.5 (4.7)	22.6 (1.4)	3.7 (0.1)	68.1 (4.7)	68.3 (3.9)	89.3 (2.2)	7.12 (0.03)
	4.94	33.9 (1.8)	49.1 (1.3)	2.4 (0.1)	72.1 (2.1)	72.1 (0.2)	125.2 (4.1)	29.6 (1.1)	3.4 (0.1)	91.6 (3.6)	88.3 (3.8)	96.5 (3.6)	7.02 (0.02)
	9.32	13.8 (2.9)	37.9 (3.9)	2.7 (0.2)	79.7 (7.5)	72.4 (0.8)	129.1 (3.4)	27.7 (1.1)	3.6 (0)	101.4 (4.3)	88 (3.6)	93.4 (1.1)	7.05 (0.03)
	22.21	7.2 (0.8)	27.1 (0.8)	3.7 (0.1)	100.6 (1.5)	107.4 (0.2)	128.7 (3.6)	28.7 (0.8)	3.6 (0.1)	105.2 (3.3)	91.4 (5.1)	88.8 (1.9)	6.93 (0.04)
	27.26	7 (0.8)	26.5 (1.2)	3.7 (0.1)	101.7 (2.3)	109.1 (0.3)	142.4 (16.6)	25.2 (0.6)	3.8 (0)	91.1 (2.3)	78.3 (3.3)	97.6 (10.5)	6.96 (0.02)

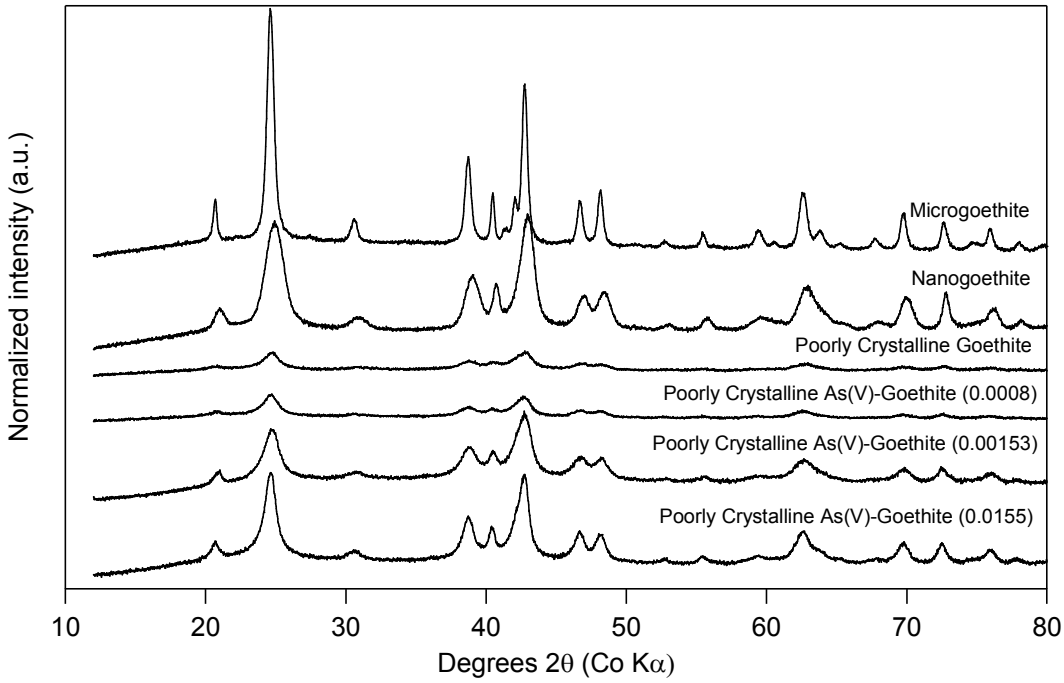

Figure 4 Powder X-ray diffraction patterns of the goethite and As(V)-goethite coprecipitates used in this study.

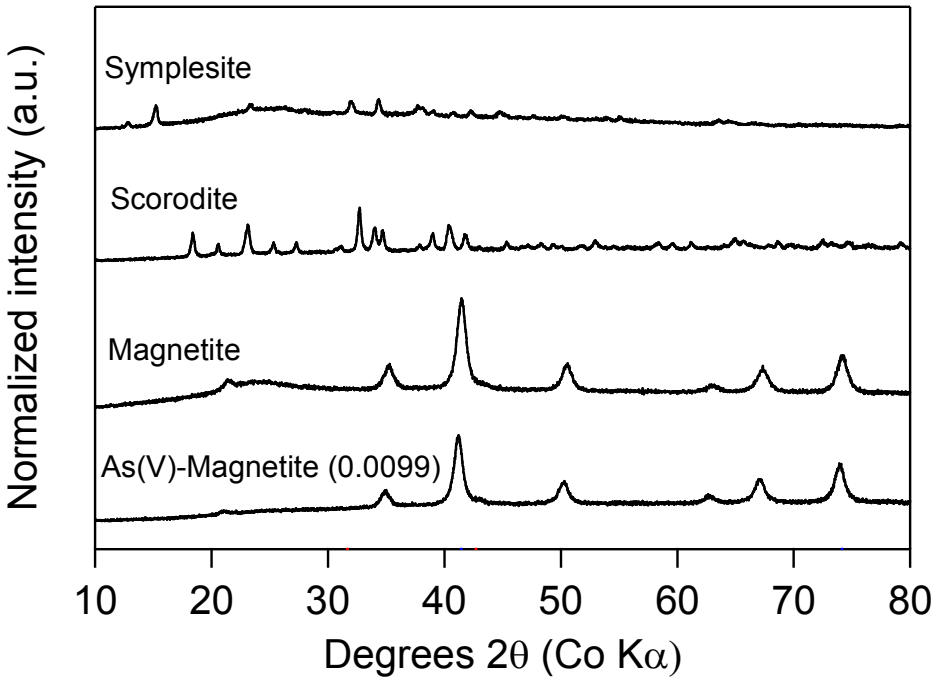

Figure 5 Powder X-ray diffraction pattern of the magnetite and As(V)-magnetite coprecipitate used in this study as compared with patterns for symplesite ($Fe^{II}_3(AsO_4)_2.8(H_2O)$) and scorodite ($Fe^{III}AsO_4.2(H_2O)$).

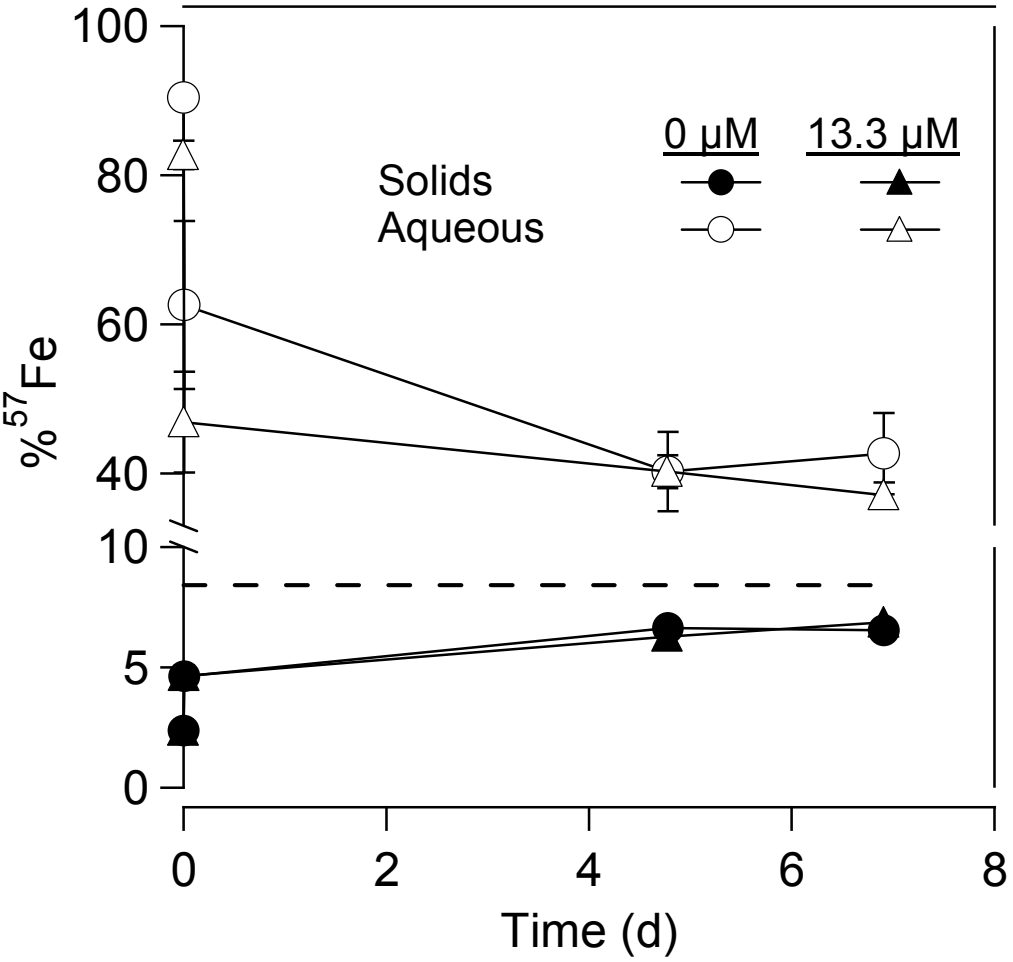

Figure 6 Fe isotope exchange between an enriched aqueous $^{57}Fe(II)$ tracer and 1 g L^{-1} magnetite in 50 mM MOPS at pH 7.2 in the presence and absence of 13.3 µM As(V).

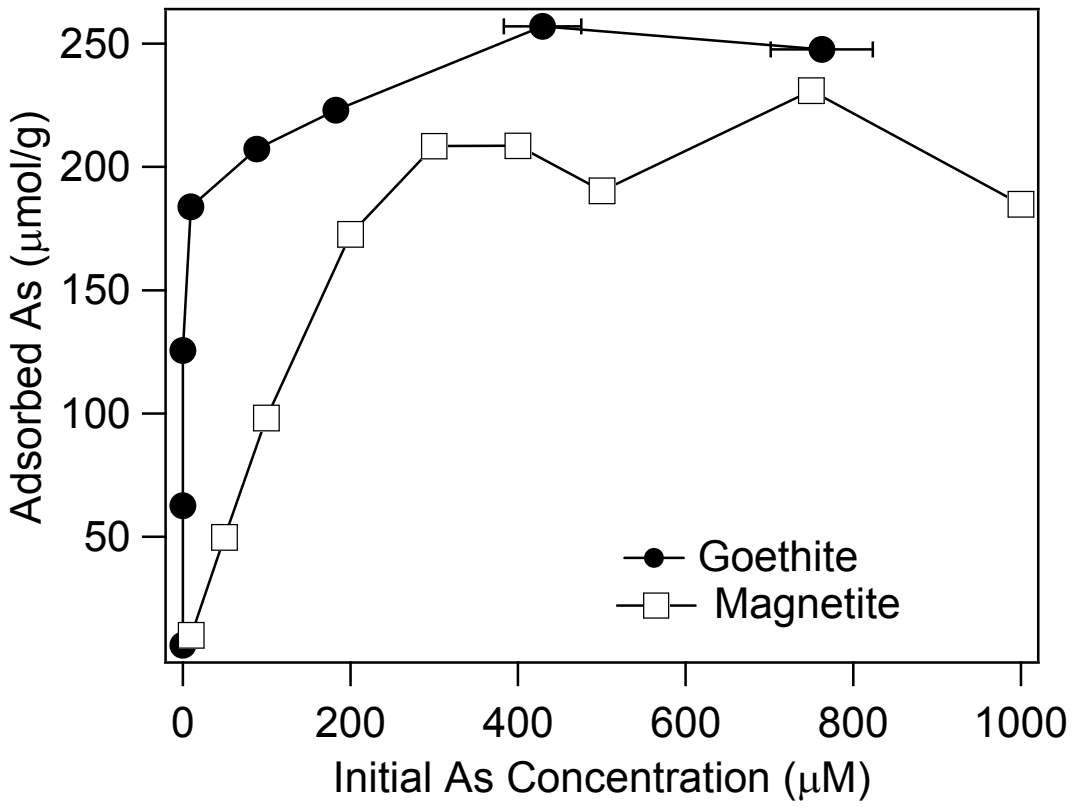

Figure 7 As(V) adsorption isotherm on magnetite (solids loading 1 g/L) buffered at pH 7.2 with 50 mM MOPS and nanogoethite (solids loading 2 g/L) buffered at pH 7.5 with 25 mM HEPES/KBr .

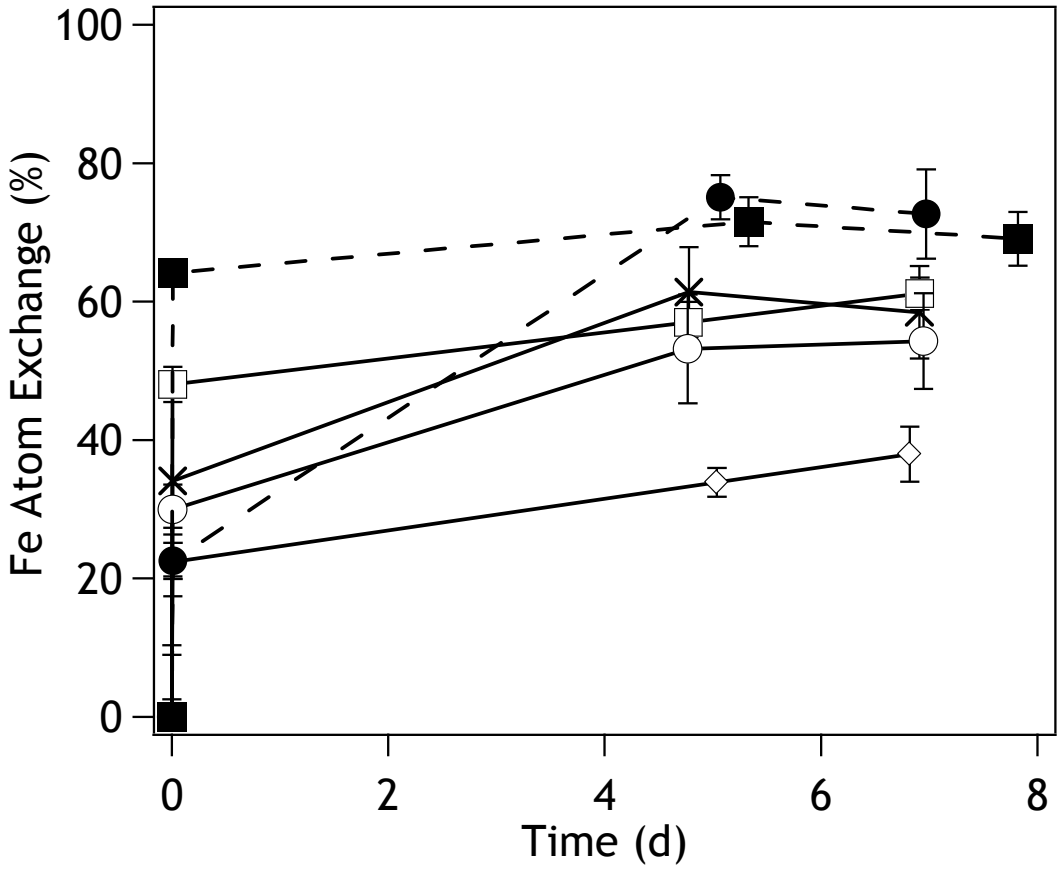

Figure 8 Effect of coprecipitated As(V) at As:Fe mole ratios of 0.005 (■) and 0.0099 (●) and adsorbed As(V) at concentrations of 0 (×), 13.3 (□), 100 (○), and 200 (◇) μM on rates of Fe(II)-catalyzed Fe atom exchange of 1 gL^{-1} magnetite in 50 mM MOPS at pH 7.2.

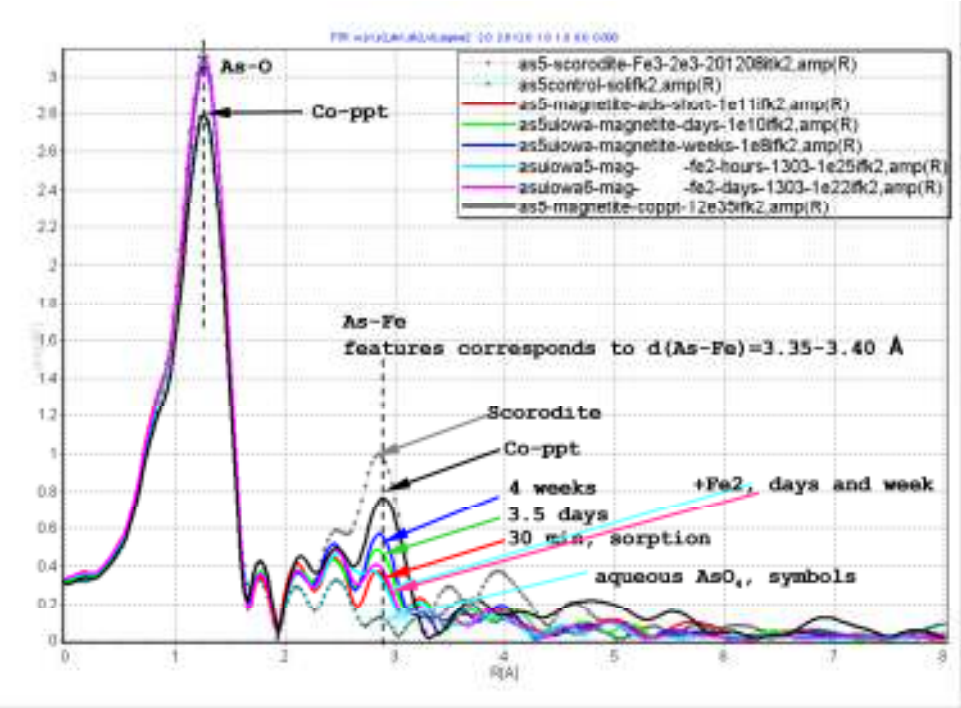

Figure 9 Fourier transforms of data from magnetite with 300 µmol/g adsorbed As(V) in the presence and absence of 1 mM Fe(II) and magnetite with coprecipitated As(V) at an initial As:Fe mole ratio of 0.007 (lines) compared to standards (symbols). Adsorption reactions were conducted at a 10 gL^{-1} magnetite loading in 50 mM MOPS at pH 7.2.

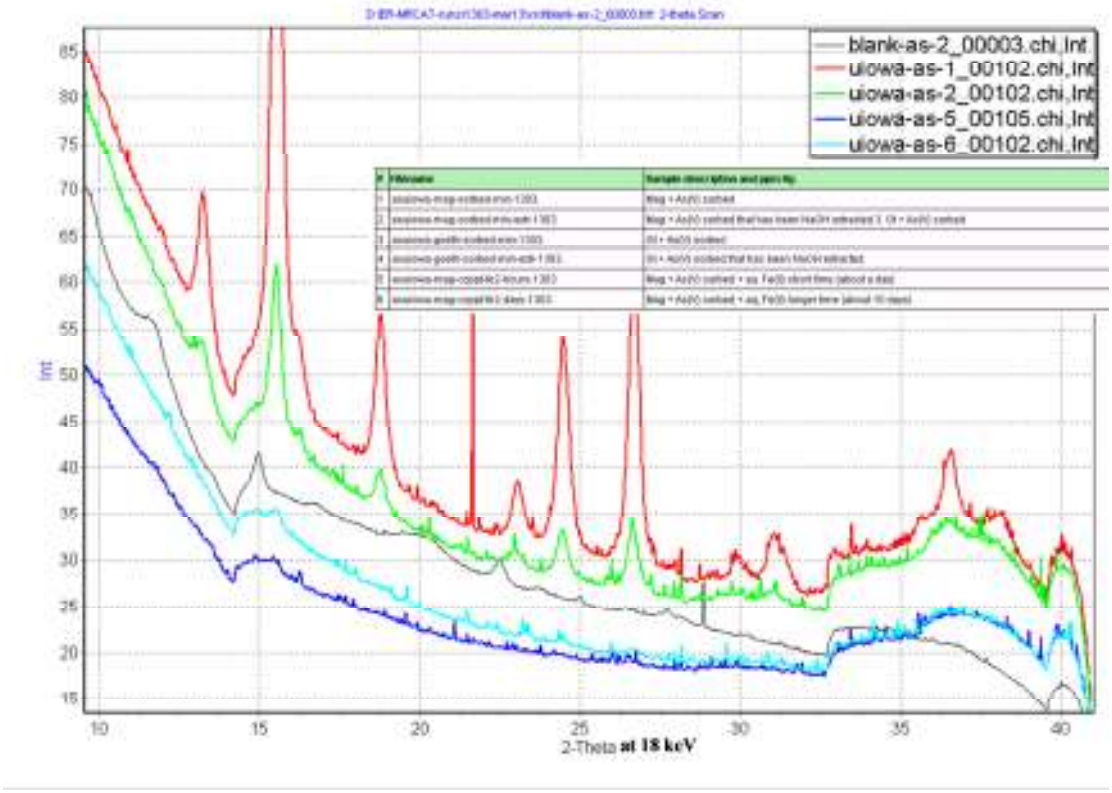

Figure 10 pXRD data for magnetite reacted with 300 µmol/g As(V) in the presence and absence of 1 mM Fe(II). All reactions were conducted at a 10 gL^{-1} magnetite loading in 50 mM MOPS at pH 7.2. The thin black line is the blank sample holder. All patterns were measured on 3 mm thick samples in transmission.

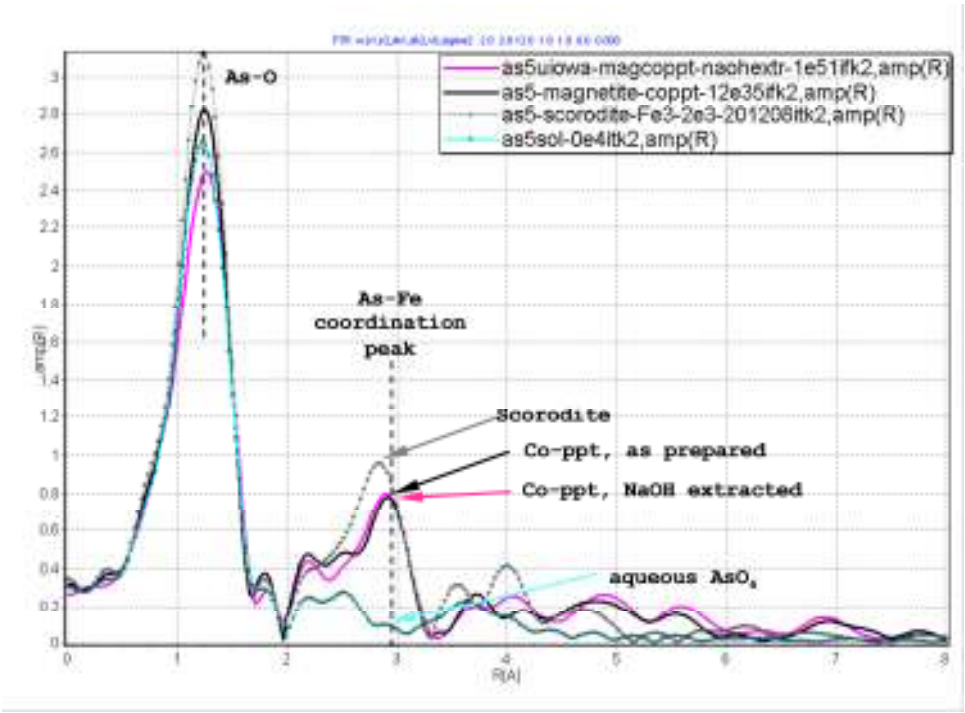

Figure 11 Fourier transforms of data from magnetite coprecipitated with As(V) at an initial As:Fe mole ratio of 0.007 before and after extracting with NaOH (lines) compared to standards (symbols).

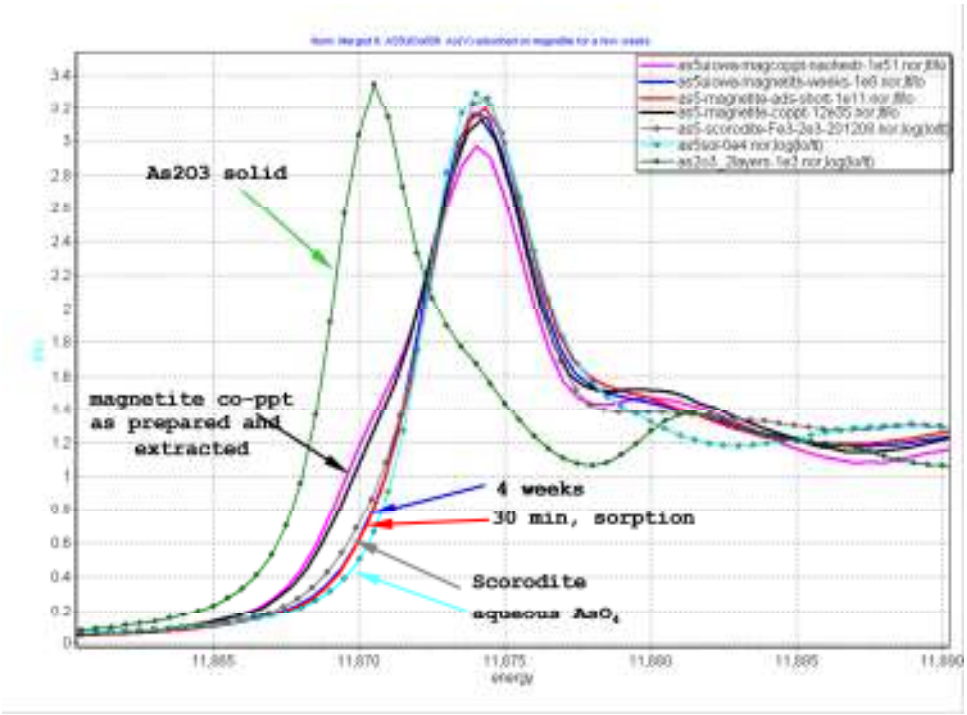

Figure 12 XANES data from magnetite with adsorbed 300 µmol/g As(V) and magnetite with coprecipitated As(V) at an initial As:Fe mole ratio of 0.007 (lines) compared to standards (symbols). Adsorption reactions were conducted at a 10 gL^{-1} magnetite loading in 50 mM MOPS at pH 7.2.

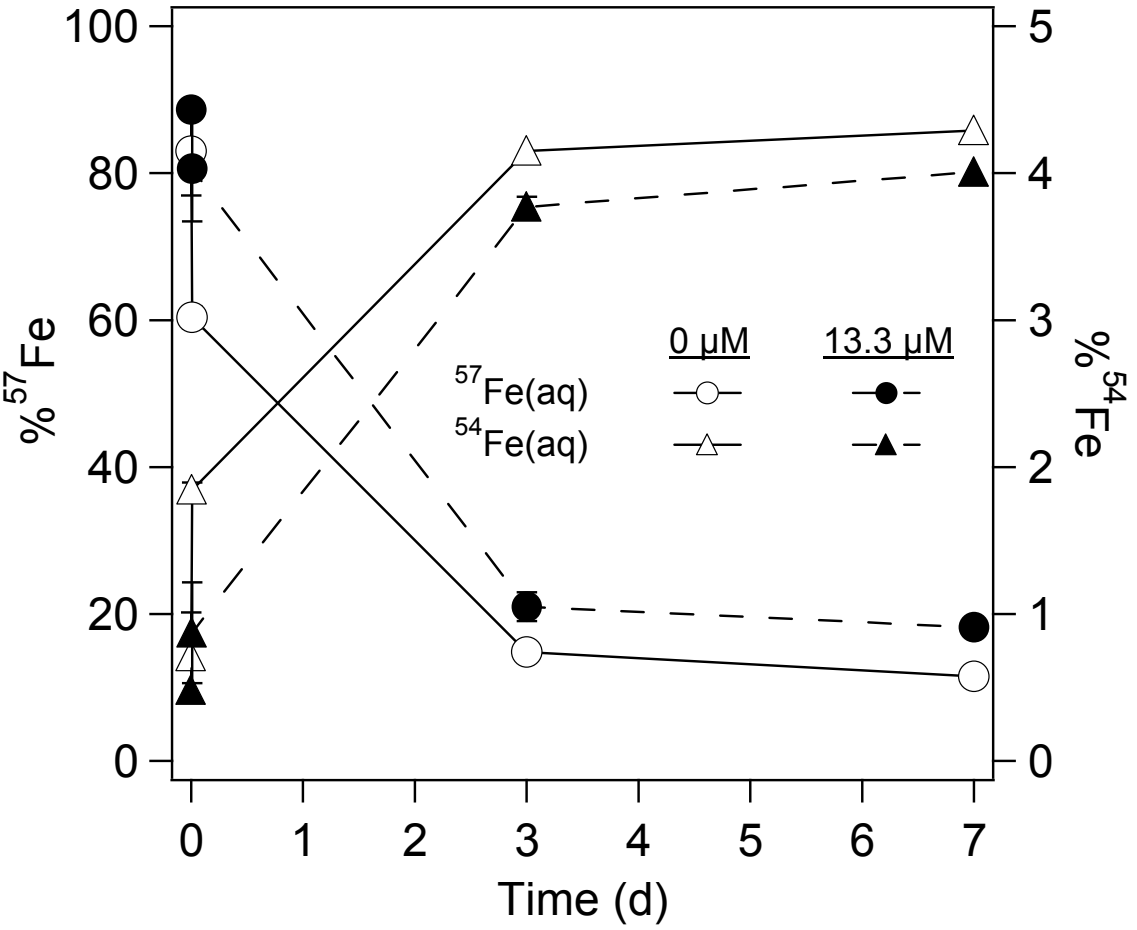

Figure 13 . Fe isotope exchange between an enriched aqueous $^{57}Fe(II)$ tracer and 2 g L^{-1} goethite in 25 mM HEPES/25 mM KBr at pH 7.5 in the presence and absence of 13.3 µM As(V).

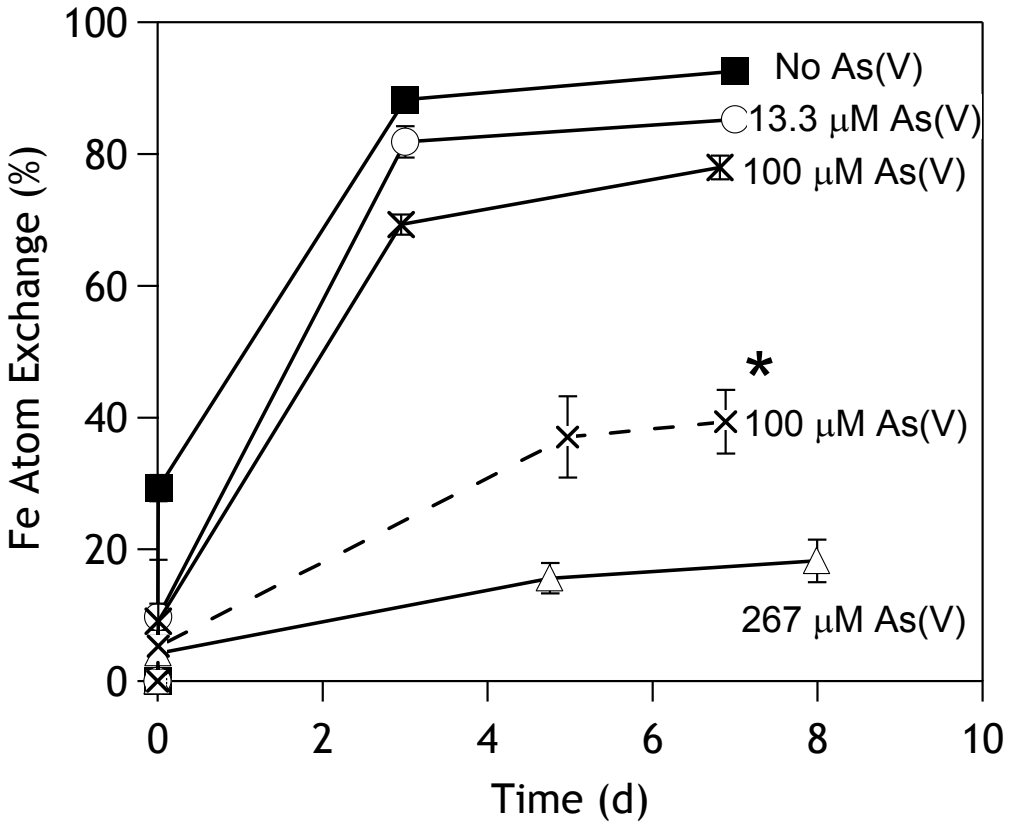

Figure 14 Effect of arsenate on rates of Fe(II)-catalyzed Fe atom exchange of 2 g L^{-1} nanogoethite in 25 mM HEPES/25 mM KBr at pH 7.5. *Conditions consistent with Catalano *et al.* (*44*) (i.e. 4 g L^{-1} microgoethite in 1 mM MES at pH 6).

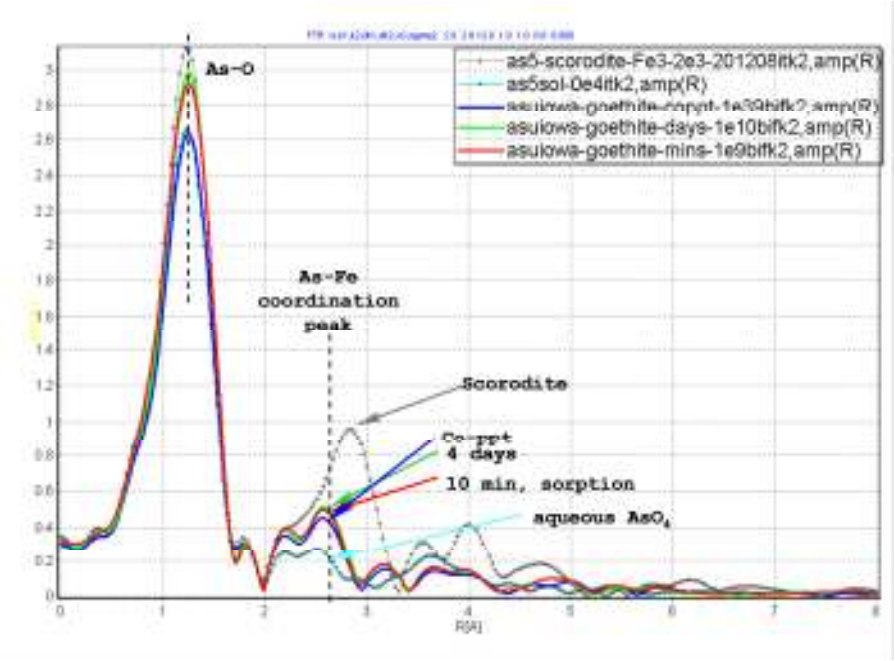

Figure 15 Fourier transforms of data from goethite with 250 µmol/g adsorbed As(V) and goethite with coprecipitated As(V) at an initial As:Fe mole ratio of 0.01 (lines) compared to standards (symbols). Adsorption reactions were conducted at a 10 gL^{-1} goethite loading in 25 mM PIPES at pH 6.5.

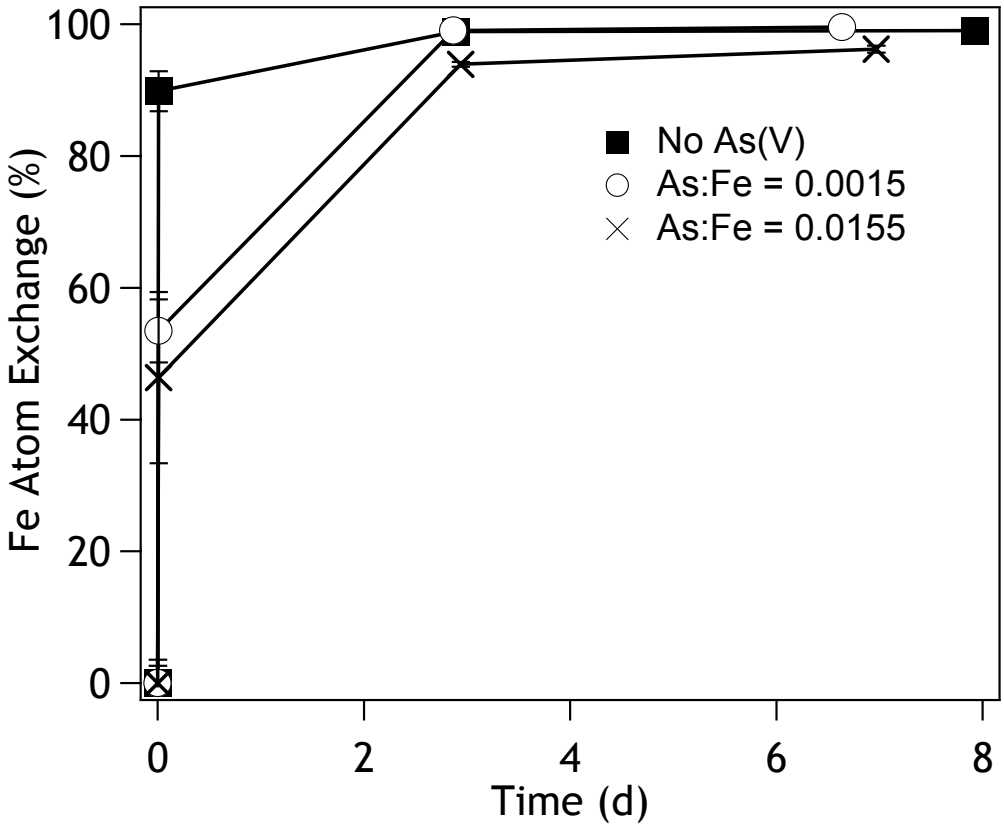

Figure 16 Effect of coprecipitated As(V) on rates of Fe(II)-catalyzed Fe atom exchange of 2 g L^{-1} goethite in 25 mM HEPES + 25 mM KBr at pH 7.5.

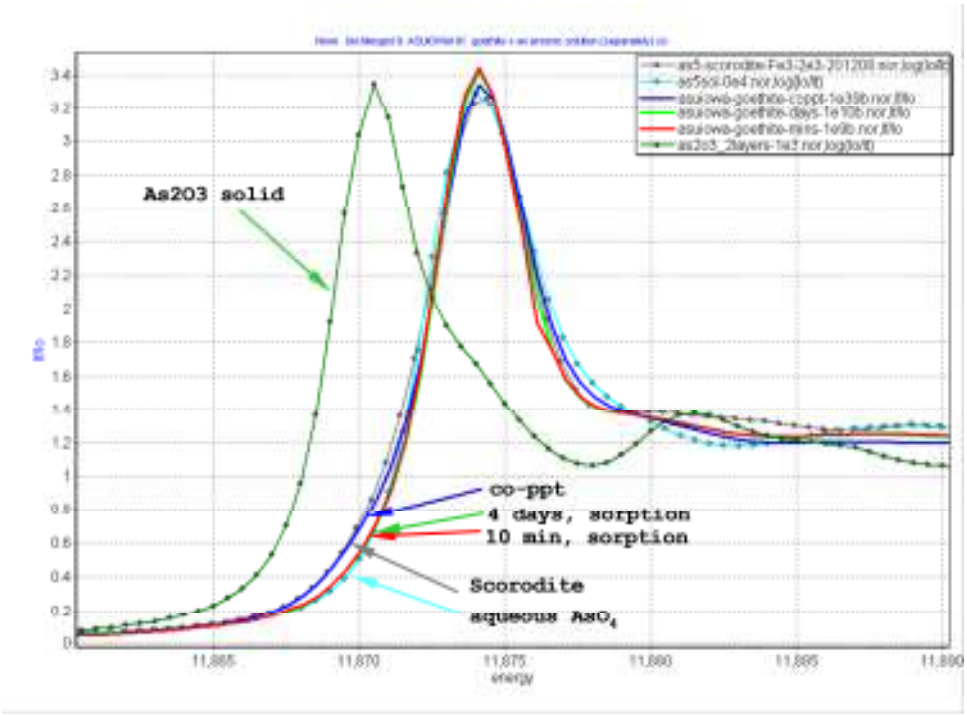

Figure 17 XANES data from goethite with 250 µmol/g adsorbed As(V) and goethite with coprecipitated As(V) at an initial As:Fe mole ratio of 0.01 (lines) compared to standards (symbols). Adsorption reactions were conducted at a 10 gL^{-1} goethite loading in 25 mM PIPES at pH 6.5.

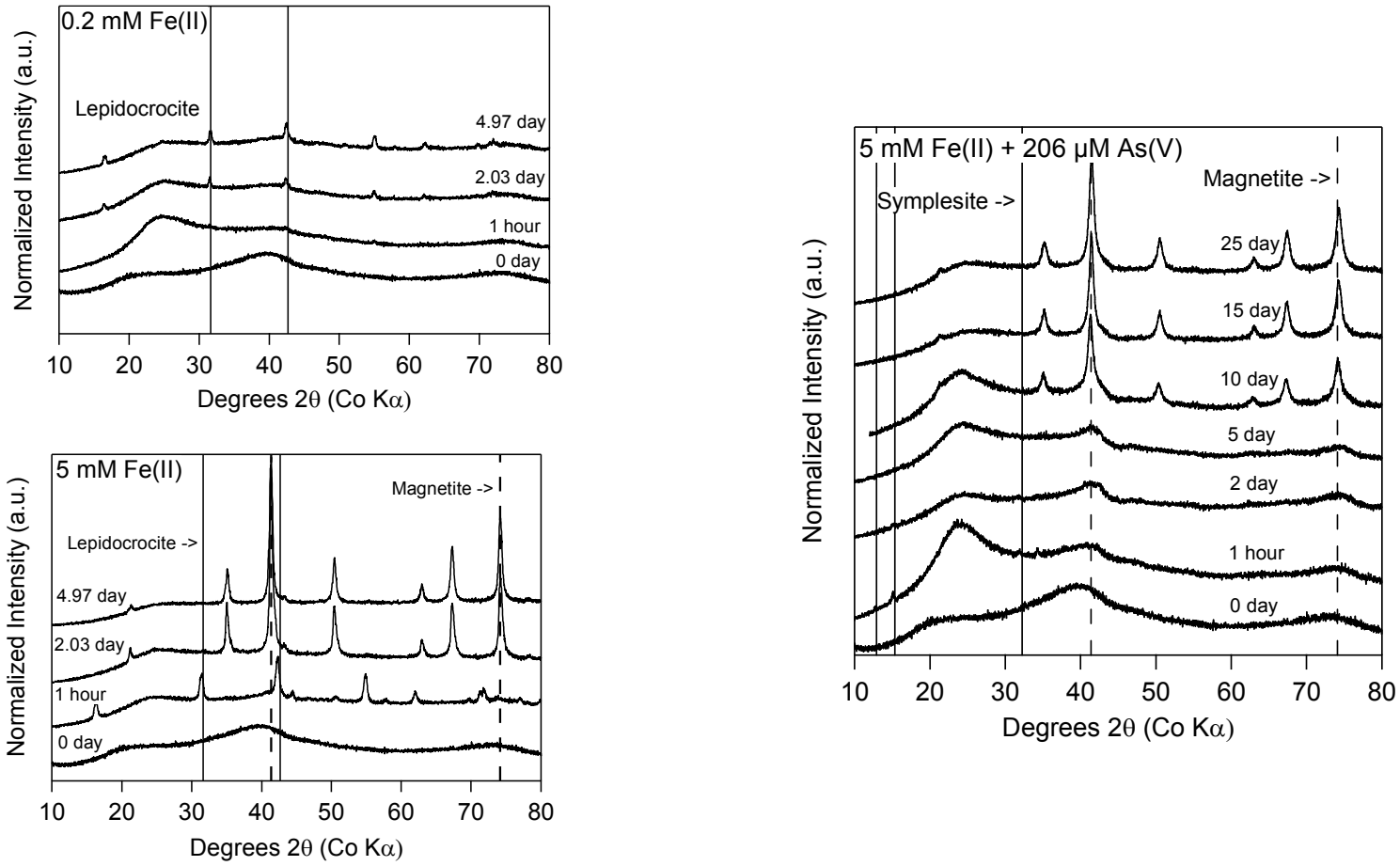

Figure 18 pXRD data demonstrating the effect of As(V) and Fe(II) concentration on the transformation of ferrihydrite 1 gL^{-1} ferrihydrite in 50 mM MOPS at an initial pH of 7.2.

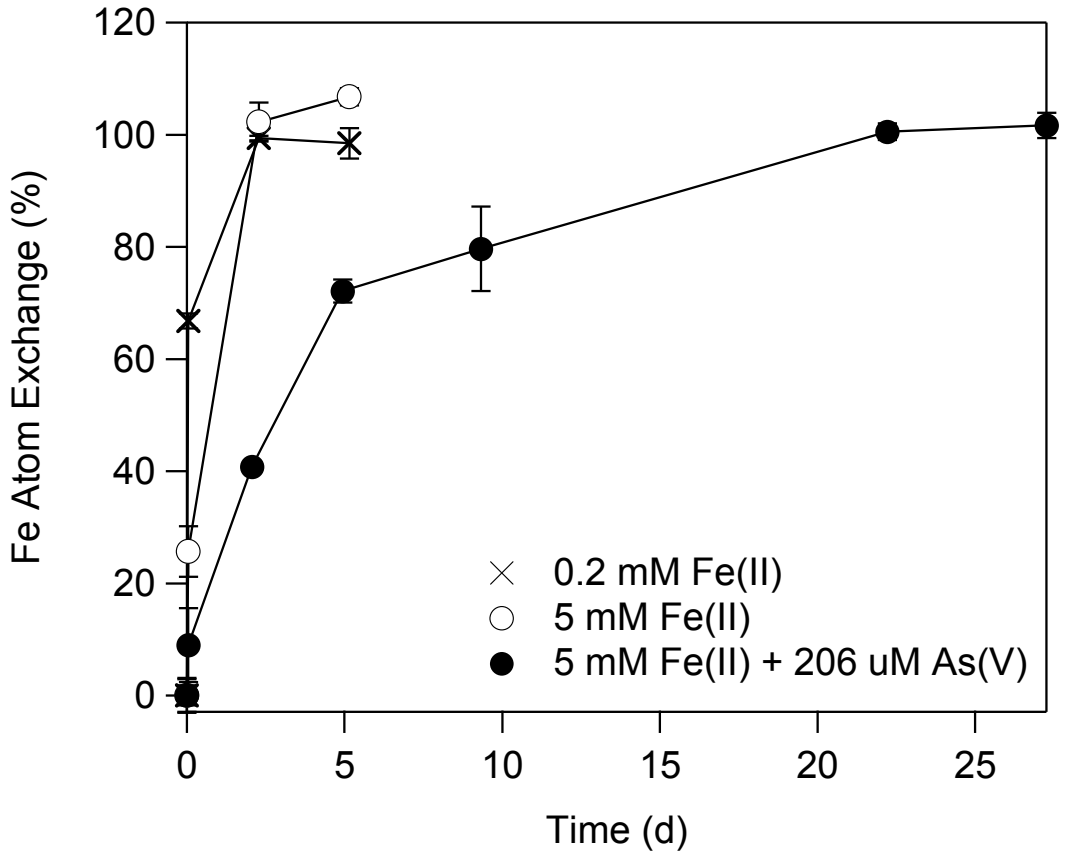

Figure 19 Effect of Fe(II) concentration and arsenate on rates of Fe(II)-catalyzed Fe atom exchange of 1 gL^{-1} ferrihydrite in 50 mM MOPS at an initial pH of 7.2.

CHAPTER III: ENGINEERING AND SCIENTIFIC SIGNIFICANCE

Summary

In this work, we demonstrated that low concentrations of adsorbed As(V) (≤ 13.3 μM) had little influence on the rate or extent of Fe(II)-catalyzed Fe atom exchange in goethite or magnetite, whereas Fe atom exchange was increasingly inhibited as As(V) concentration increased above 100 μM. We showed that adsorbed As(V) may be incorporated into magnetite in the presence and absence of added Fe(II). We also demonstrated that As(V) may be incorporated into goethite and magnetite during their precipitation, and that coprecipitated As(V) at the As:Fe ratios of this study (0.0005-0.0155) did not inhibit atom exchange. Atom exchange data indicated that ferrihydrite likely transforms via a dissolution-reprecipitation mechanism both to lepidocrocite at 0.2 mM Fe(II) and to magnetite at 5 mM Fe(II). Although the presence of 206 μM As(V) slowed both ferrihydrite transformation and atom exchange, a comparison of atom exchange and XRD patterns show that the degree of atom exchange between aqueous Fe(II) and ferrihydrite does not directly correlate with the amount of ferrihydrite transformed.

Outlook and Recommendations for Future Work

The work presented here indicates that high concentrations of As(V) can inhibit the Fe(II)-catalyzed recrystallization of Fe oxides. This has implications for the fate and transport of As and other contaminants, since Fe(II)-catalyzed recrystallization can lead to the uptake and release of many trace metals (*43*). We also observe that As(V) may be incorporated into magnetite over timescales of several days to weeks both in the presence and absence of Fe(II). This suggests that As(V) uptake and release by magnetite may be an overlooked mechanism of As(V) sequestration or mobilization in the environment.

Further work is needed to better constrain the kinetics of As(V) uptake by magnetite in the presence and absence of Fe(II). This work should determine on what

timescales arsenic is incorporated into magnetite and whether the rate of incorporation is affected by the concentration of Fe(II) in the system. Additional XAS studies could also determine whether the structural environment of As(V) in the magnetite solid is affected by Fe(II) concentration in solution or reaction time. Similarly, XAS, chemical extraction, and atom exchange studies should be coupled to determine whether coprecipitated As(V) is redistributed from the magnetite structure to the magnetite surface over time during Fe(II)-catalyzed recrystallization.

More work is also needed to determine whether adsorbed As(V) is incorporated into goethite or into the transformation products of ferrihydrite in the presence of Fe(II). Prior research has suggested that As(V) is incorporated into the products of the Fe(II)-catalyzed transformation of lepidocrocite and ferrihydrite based on chemical extraction data (*68*). Future work along these lines could determine the speciation and bonding environment of the arsenic using XAS, and could couple these observations with chemical extractions of the arsenic and atom exchange measurements to identify changes in arsenic mobility over the course of a reaction.

Finally, our observations of ferrihydrite transformation at two different Fe(II) concentrations and in the presence of As(V) raise many additional questions. It would be worthwhile to do a comprehensive study of how varying concentrations of As(V) affect both Fe atom exchange and the end products of ferrihydrite transformation. It would be interesting to observe whether changes in transformation mechanism (as measured by changes in the observed extent of atom exchange) could be correlated to changes in transformation products. It would also be interesting to measure atom exchange during ferrihydrite transformation at a range of Fe(II) concentrations for both 6-line and 2-line ferrihydrite, and in the presence and absence of additional common groundwater components such as carbonate, in order to determine the effect of the concentrations of Fe(II) and of other common ions on ferrihydrite transformation mechanisms and products. This exploration of controls on ferrihydrite transformation could have

important implications for the uptake and release of many groundwater contaminants under natural groundwater conditions. It is also relevant to understanding controls on contaminant mobility during human-induced redox cycling of groundwater, such as occurs during aquifer storage and recovery (*73*, *74*) and could lead to an improved understanding of arsenic uptake and removal in iron oxide-based point-of-use arsenic removal systems.

REFERENCES

(1) Hughes, J. B.; Wang, C.; Rudolph, F. Bamberger Rearrangement during TNT Metabolism by Clostridium acetobutylicum. *Environmental Science & Technology* **1998**, *32*, 494.

(2) Saha, J. C.; Dikshit, a. K.; Bandyopadhyay, M.; Saha, K. C. A Review of Arsenic Poisoning and its Effects on Human Health. *Critical Reviews in Environmental Science and Technology* **1999**, *29*, 281–313.

(3) Bissen, M.; Frimmel, F. H.; Ag, C. Arsenic – a Review . Part I : Occurrence , Toxicity , Speciation , Mobility. **2003**, *31*, 9–18.

(4) Smedley, P. .; Kinniburgh, D. . A review of the source, behaviour and distribution of arsenic in natural waters. *Applied Geochemistry* **2002**, *17*, 517–568.

(5) Welch, A.; Westjohn, D.; Helsel, D.; Wanty, R. Arsenic in ground water of the United States: occurrence and geochemistry. http://water.usgs.gov/nawqa/trace/pubs/gw_v38n4/ (accessed March 3, 2013).

(6) Levine, T.; Rispin, A.; Siegel Scott, C.; Marchus, W.; Chen, C.; Gibb, H. Special Report on Ingested Inorganic Arsenic - Skin Cancer ; Nutritional Essentiality **1988**, 124 p.

(7) Bowell, R. J. Sorption of arsenic by iron oxides and hydroxides in soils. *Applied Geochemistry* **1994**, *9*, 279–286.

(8) BGS; DPHE Arsenic contamination of groundwater in Bangladesh. In; Kinniburgh, D. G.; Smedley, P. ., Eds.; British Geological Survey: Keyworth, 2001; Vol. 3.

(9) Pichler, T.; Veizer, J. A. N.; Hall, G. E. M. Natural Input of Arsenic into a Coral-Reef Ecosystem by Hydrothermal Fluids and Its Removal by Fe (III) Oxyhydroxides. **1999**, *33*, 1373–1378.

(10) Smedley, P. L.; Kinniburgh, D. G. A review of the source , behaviour and distribution of arsenic in natural waters. **2002**, *17*, 517–568.

(11) Weber, K. a; Achenbach, L. a; Coates, J. D. Microorganisms pumping iron: anaerobic microbial iron oxidation and reduction. *Nature reviews. Microbiology* **2006**, *4*, 752–64.

(12) Lovley, D. R.; Phillips, E. J. P. Novel Mode of Microbial Energy-Metabolism - Organic-Carbon Oxidation Coupled to Dissimilatory Reduction of Iron or Manganese. *Appl. Environ. Microbiol.* **1988**, *54*, 1472–1480.

(13) Kocar, B. D.; Herbel, M. J.; Tufano, K. J.; Fendorf, S. Contrasting effects of dissimilatory iron (III) and arsenic (V) reduction on arsenic retention and transport. *Environmental science & technology* **2006**, *40*, 6715–21.

(14) VanCappellen, P.; Wang, Y. F.; Van Cappellen, P. Cycling of iron and manganese in surface sediments: A general theory for the coupled transport and raction of carbon, oxygen, nitrogen, sulfur, iron and manganese. *American Journal of Science* **1996**, *296*, 197–243.

(15) Cornell, R. M.; Schwertmann, U. *The Iron Oxides: Structure, Properties, Reactions, Occurrence, and Uses*; VCH: New York, 1996.

(16) Vikesland, P. J.; Heathcock, A. M. A. P.; Rebodos, R. L.; Makus, K. E. Particle size and aggregation effects on magnetite reactivity toward carbon tetrachloride. *Environmental Science and Technology* **2007**, *41*, 5277–5283.

(17) Peterson, M. L.; White, A. F.; Brown, G. E.; Parks, G. A. Surface passivation of magnetite by reaction with aqueous Cr(VI): XAFS and TEM results. *Environmental Science & Technology* **1997**, *31*, 1573–1576.

(18) Gorski, C. A.; Scherer, M. M. Influence of Magnetite Stoichiometry on Fe II Uptake and Nitrobenzene Reduction. *Environmental Science & Technology* **2009**, *43*, 3675–3680.

(19) Hansel, C. M. C. M.; Benner, S. G. S. G.; Fendorf, S. Competing Fe(II)-Induced Mineralization Pathways of Ferrihydrite. *Environmental Science & Technology* **2005**, *39*, 7147–7153.

(20) Das, S.; Hendry, M. J.; Essilfie-Dughan, J. Transformation of two-line ferrihydrite to goethite and hematite as a function of pH and temperature. *Environmental science & technology* **2011**, *45*, 268–75.

(21) Tamaura, Y.; Ito, K.; Katsura, T. Transformation of y-FeO(OH) to Fe3O4 by Adsorption of Iron(II) Ion on y-FeO(OH). *Chem. Soc. Dalton Trans.* **1983**, 189–194.

(22) Williams, A. G. B.; Scherer, M. M. Spectroscopic evidence for Fe (II)-Fe (III) electron transfer at the iron oxide-water interface. *Environmental science & technology* **2004**, *38*, 4782–4790.

(23) Gorski, C. A.; Scherer, M. M. Influence of Magnetite Stoichiometry on FeII Uptake and Nitrobenzene Reduction. *Environmental Science & Technology* **2009**, *43*, 3675–3680.

(24) Handler, R. M.; Beard, B. L.; Johnson, C. M.; Scherer, M. M. Atom exchange between aqueous Fe (II) and goethite: An Fe isotope tracer study. *Environmental Science & Technology* **2009**, *43*, 1102–1107.

(25) Gorski, C. A.; Handler, R. M.; Beard, B. L.; Pasakarnis, T.; Johnson, C. M.; Scherer, M. M. Fe Atom Exchange between Aqueous Fe2+ and Magnetite. *Environ. Sci. Technol.* **2012**.

(26) Jones, A. M.; Collins, R. N.; Rose, J.; Waite, T. D. The effect of silica and natural organic matter on the Fe(II)-catalysed transformation and reactivity of Fe(III) minerals. *Geochimica et Cosmochimica Acta* **2009**, *73*, 4409–4422.

(27) Pedersen, H. D. *The transformation of Fe (III) oxides catalysed by Fe2+ and the fate of arsenate during transformation and reduction of Fe (III) oxides*; Institute of Environment & Resources, Technical University of Denmark, 2006.

(28) Pedersen, H. D. H. D.; Postma, D.; Jakobsen, R.; Larsen, O. Fast transformation of iron oxyhydroxides by the catalytic action of aqueous Fe(II). *Geochimica et Cosmochimica Acta* **2005**, *69*, 3967–3977.

(29) Gallagher, K. J.; Feitknecht, W.; Mannweiler, U. Mechanism of Oxidation of Magnetite to g-Fe2O3. *Nature* **1968**, *217*, 1118–1121.

(30) Tang, J.; Myers, M.; Bosnick, K. A.; Brus, L. E. Magnetite Fe3O4 nanocrystals: Spectroscopic observation of aqueous oxidation kinetics. *Journal of Physical Chemistry: B* **2003**, *107*, 7501–7506.

(31) Sidhu, P. S.; Gilkes, R. J.; Posner, A. M. Mechanism of the low temperature oxidation of magnetite. *Journal of Inorganic and Nuclear Chemistry* **1977**, *39*, 1953–8.

(32) Colombo, U.; Fagherazzi, G.; Gazzarrini, F.; Lanzavecchia, G.; Sironi, G. Mechanism of low-temperature oxidation of magnetites. *Nature* **1968**, *219*, 1036–1037.

(33) White, A. F.; Peterson, M. L.; Hochella, M. F. Electrochemistry and Dissolution Kinetics of Magnetite and Ilmenite. *Geochimica et Cosmochimica Acta* **1994**, *58*, 1859–1875.

(34) Gorski, C. a; Handler, R. M.; Beard, B. L.; Pasakarnis, T.; Johnson, C. M.; Scherer, M. M. Fe atom exchange between aqueous Fe2+ and magnetite. *Environmental science & technology* **2012**, *46*, 12399–407.

(35) Yanina, S. V. V.; Rosso, K. M. M. Linked Reactivity at Mineral-Water Interfaces Through Bulk Crystal Conduction. *Science* **2008**, *320*, 218–222.

(36) Wang, Y.; Morin, G.; Ona-Nguema, G.; Juillot, F.; Calas, G.; Brown, G. E. Distinctive arsenic(V) trapping modes by magnetite nanoparticles induced by different sorption processes. *Environmental science & technology* **2011**, *45*, 7258–66.

(37) Coker, V. S.; Gault, A. G.; Pearce, C. I.; Van der Laan, G.; Telling, N. D.; Charnock, J. M.; Polya, D. A.; Lloyd, J. R. XAS and XMCD evidence for species-dependent partitioning of arsenic during microbial reduction of ferrihydrite to magnetite. *Environmental science & technology* **2006**, *40*, 7745–7750.

(38) Nico, P. S. P. S.; Stewart, B. D. B. D.; Fendorf, S. Incorporation of Oxidized Uranium into Fe (Hydr)oxides during Fe(II) Catalyzed Remineralization. *Environmental Science & Technology* **2009**, *43*, 7391–7396.

(39) Boland, D. D.; Collins, R. N.; Payne, T. E.; Waite, T. D. Effect of Amorphous Fe(III) Oxide Transformation on the Fe(II)-Mediated Reduction of U(VI). *Environmental science & technology* **2011**, 1327–1333.

(40) Frierdich, a. J.; Luo, Y.; Catalano, J. G. Trace element cycling through iron oxide minerals during redox-driven dynamic recrystallization. *Geology* **2011**, *39*, 1083–1086.

(41) Um, W.; Chang, H.-S.; Icenhower, J. P.; Lukens, W. W.; Serne, R. J.; Qafoku, N. P.; Westsik, J. H.; Buck, E. C.; Smith, S. C. Immobilization of 99-technetium (VII) by Fe(II)-goethite and limited reoxidation. *Environmental science & technology* **2011**, *45*, 4904–13.

(42) Frierdich, A. J.; Catalano, J. G. Controls on Fe(II)-activated trace element release from goethite and hematite. *Environmental science & technology* **2012**, *46*, 1519–26.

(43) Latta, D. E.; Gorski, C. a; Scherer, M. M. Influence of Fe2+-catalysed iron oxide recrystallization on metal cycling. *Biochemical Society transactions* **2012**, *40*, 1191–7.

(44) Catalano, J. G.; Luo, Y.; Otemuyiwa, B. T. Effect of aqueous Fe (II) on arsenate sorption on goethite and hematite. *Environmental science & technology* **2011**.

(45) Kocar, B. D. B. D.; Fendorf, S. Thermodynamic Constraints on Reductive Reactions Influencing the Biogeochemistry of Arsenic in Soils and Sediments. *Environmental Science & Technology* **2009**, *43*, 4871–4877.

(46) Amstaetter, K.; Borch, T.; Larese-Casanova, P.; Kappler, A. Redox Transformation of Arsenic by Fe(II)-Activated Goethite (Î±-FeOOH). *Environmental Science & Technology* **2009**, *44*, 102–108.

(47) Monitoring, W.; Section, A. Iowa Statewide Rural Well Water Survey Phase 2 (SWRL2) Results and Analysis. **2009**, *2*.

(48) Burleson, D. J.; Penn, R. L. Two-step growth of goethite from ferrihydrite. *Langmuir* **2006**, *22*, 402–409.

(49) Cwiertny, D. M.; Handler, R. M.; Schaefer, M. V.; Grassian, V. H.; Scherer, M. M. Interpreting nanoscale size-effects in aggregated Fe-oxide suspensions: reaction of Fe (II) with goethite. *Geochimica et Cosmochimica Acta* **2008**, *72*, 1365–1380.

(50) Catalano, J. G.; Luo, Y.; Otemuyiwa, B. Effect of aqueous Fe(II) on arsenate sorption on goethite and hematite. *Environmental science & technology* **2011**, *45*, 8826–33.

(51) Schwertmann, U.; Cornell, R. M. *Iron Oxides in the Laboratory: Preparation and Characterization*; Wiley-VCH: New York, 2000; Vol. 2nd, p. 188.

(52) Pedersen, H. D. D.; Postma, D.; Jakobsen, R. Release of arsenic associated with the reduction and transformation of iron oxides. *Geochimica et Cosmochimica Acta* **2006**, *70*, 4116–4129.

(53) Gorski, C. A.; Scherer, M. M. Influence of Magnetite Stoichiometry on Fe(II) Uptake and Nitrobenzene Reduction. *Environ Sci Technol Environ Sci Technol* **2009**, *43*, 3675–3680.

(54) Gorski, C. A. A.; Scherer, M. M. M. Determination of nanoparticulate magnetite stoichiometry by Mossbauer spectroscopy, acidic dissolution, and powder X-ray diffraction: A critical review. *American Mineralogist* **2010**, *95*, 1017–1026.

(55) Wang, Y.; Morin, G.; Ona-Nguema, G.; Juillot, F.; Calas, G.; Brown Jr, G. E. Distinctive Arsenic (V) Trapping Modes by Magnetite Nanoparticles Induced by Different Sorption Processes. *Environmental science & technology* **2011**.

(56) Wilkie, J. A.; Hering, J. G. Adsorption of arsenic onto hydrous ferric oxide: effects of adsorbate/adsorbent ratios and co-occurring solutes. *Colloids and Surfaces A: Physicochemical and Engineering Aspects* **1996**, *107*, 97–110.

(57) Tamura, H.; Goto, K.; Yotsuyan.T; Nagayama, M. Spectrophotometric Determination of Iron(II) with 1,10-Phenanthroline in Presence of Large Amounts of Iron(III). *Talanta* **1974**, *21*, 314–318.

(58) Brown, R. J. C.; Yardley, R. E.; Brown, A. S.; Milton, M. J. T. Sample matrix and critical interference effects on the recovery and accuracy of concentration measurements of arsenic in ambient particulate samples using ICP-MS. *Journal of Analytical Atomic Spectrometry* **2004**, *19*, 703.

(59) Cai, Y.; Georgiadis, M.; Fourqurean, J. W. Determination of arsenic in seagrass using inductively coupled plasma mass spectrometry. *Spectrochimica Acta Part B: Atomic Spectroscopy* **2000**, *55*, 1411–1422.

(60) Masue-Slowey, Y.; Loeppert, R. H.; Fendorf, S. Alteration of ferrihydrite reductive dissolution and transformation by adsorbed As and structural Al: Implications for As retention. *Geochimica et Cosmochimica Acta* **2011**, *75*, 870–886.

(61) Jönsson, J.; Sherman, D. M. M.; Jonsson, J. Sorption of As(III) and As(V) to siderite, green rust (fougerite) and magnetite: Implications for arsenic release in anoxic groundwaters. *Chemical Geology* **2008**, *255*, 173–181.

(62) Latta, D. E.; Bachman, J. E.; Scherer, M. M. Fe electron transfer and atom exchange in goethite: influence of Al-substitution and anion sorption. *Environmental science & technology* **2012**, *46*, 10614–23.

(63) Frierdich, A. J.; Luo, Y.; Catalano, J. G. Trace element cycling through iron oxide minerals during redox-driven dynamic recrystallization. *Geology* **2011**, *39*, 1083–1086.

(64) Jönsson, J.; Sherman, D. M. Sorption of As (III) and As (V) to siderite, green rust (fougerite) and magnetite: Implications for arsenic release in anoxic groundwaters. *Chemical Geology* **2008**, *255*, 173–181.

(65) Dixit, S.; Hering, J. G. Comparison of arsenic(V) and arsenic(III) sorption onto iron oxide minerals: Implications for arsenic mobility. *Environmental Science & Technology* **2003**, *37*, 4182–4189.

(66) Hiemstra, T.; Van Riemsdijk WH Surface Structural Ion Adsorption Modeling of Competitive Binding of Oxyanions by Metal (Hydr)oxides. *Journal of colloid and interface science* **1999**, *210*, 182–193.

(67) Sherman, D. M.; Randall, S. R. Surface complexation of arsenic(V) to iron(III) (hydr)oxides: structural mechanism from ab initio molecular geometries and EXAFS spectroscopy. *Geochimica et Cosmochimica Acta* **2003**, *67*, 4223–4230.

(68) Pedersen, H. D.; Postma, D.; Jakobsen, R. Release of arsenic associated with the reduction and transformation of iron oxides. *Geochimica et Cosmochimica Acta* **2006**, *70*, 4116–4129.

(69) Yang, L.; Steefel, C. I. I.; Marcus, M. A. A.; Bargar, J. R. R. Kinetics of Fe(II)-Catalyzed Transformation of 6-line Ferrihydrite under Anaerobic Flow Conditions. *Environ. Sci. Technol.* **2010**, *44*, 5469–5475.

(70) Jones, A. M.; Collins, R. N.; Rose, J.; Waite, T. D. The effect of silica and natural organic matter on the Fe(II)-catalysed transformation and reactivity of Fe(III) minerals. *Geochim. Cosmochim. Acta* **2009**, *73*, 4409–4422.

(71) Masue-Slowey, Y.; Loeppert, R. H. R. H. H.; Fendorf, S. Alteration of ferrihydrite reductive dissolution and transformation by adsorbed As and structural Al: Implications for As retention. *Geochimica et Cosmochimica Acta* **2011**, *75*, 870–886.

(72) Das, S.; Hendry, M. J.; Essilfie-Dughan, J. Effects of adsorbed arsenate on the rate of transformation of 2-line ferrihydrite at pH 10. *Environmental science & technology* **2011**, *45*, 5557–63.

(73) Arthur, J. D.; Dabous, A. A.; Cowart, J. B. Mobilization of arsenic and other trace elements during aquifer storage and recovery, southwest Florida. In *U.S. Geological Survey Artificial Recharge Workshop Proceedings*; Aiken, G. R.; Kunianski, E. L., Eds.; Sacramento, CA, 2002.

(74) Wallis, I.; Prommer, H.; Pichler, T.; Post, V.; Norton, S. B.; Annable, M. D.; Simmons, C. T. Process-based reactive transport model to quantify arsenic mobility during aquifer storage and recovery of potable water. *Environmental science & technology* **2011**, *45*, 6924–31.